Supporting Information

Spongy Materials Based on Supramolecular Polymer Networks for Detection and Separation of Broad Spectrum Pollutants

Qi Lin,*,† Xiao-Wen Guan,† You-Ming Zhang,*,†,‡ Jiao Wang,† Yan-Qing Fan,† Hong Yao,†

Tai-Bao Wei*,†

†Qi Lin, Xiao-Wen Guan, Jiao Wang, Yan-Qing Fan, Hong Yao, Tai-Bao Wei. Key Laboratory of Eco-Environment-Related Polymer Materials, Ministry of Education of China; Research Center of Gansu Military and Civilian Integration Advanced Structural Materials; College of Chemistry and Chemical Engineering, Northwest Normal University, Lanzhou, 730070, China; E-mail: linqi2004@126.com; weitaibao@126.com.

‡ You-Ming Zhang. College of Chemistry and Chemical Engineering, Lanzhou City University, Lanzhou, Gansu, 730070, China; E-mail: zhangnwnu@126.com.

Suporting Informaltion:

Number of pages: 37 (S1–S37)

Number of Figure: 45 (Figure S1–S45)

Number of Table: 6 (Table S1-S6)

Table of Contents

Materials and instruments

All cations were used as the perchlorate salts, while all anions were used as the sodium salts, which were purchased from Alfa Aesar and used as received. All dyes were used as the analytical purity, which purchased from Aladdin. Fresh double distilled water was used throughout the experiment. Nuclear magnetic resonance (NMR) spectra were recorded on Varian Mercury 400 and Varian Inova 600 instruments. Mass spectra were recorded on a Bruker Esquire 6000 MS instrument. The X-ray diffraction analysis (XRD) was performed in a transmission mode with a Rigaku RINT2000 diffractometer equipped with graphite monochromated CuKa radiation (λ = 1.54073 Å). The morphologies and sizes of the xerogels were characterized using field emission scanning electron microscopy (FE-SEM, JSM-6701F) at an accelerating voltage of 8 kV. The infrared spectra were performed on a Digilab FTS-3000 Fourier transform-infrared spectrophotometer. Melting points were measured on an X-4 digital melting-point apparatus (uncorrected). Fluorescence spectra were recorded on a Shimadzu RF-5301PC spectrofluorophotometer. Ultraviolet-visible (UV-vis) spectra were recorded on a Shimadzu UV-2550 spectrometer. Thermogravimetric Analysis (TGA) was carried out on a DSCQ1000 Thermal Gravimetric Analyzer. Surface area measurements were conducted on a BELSORP-Max Accelerated Surface Area and Porosimetry Analyzer. The sample was degassed at 100 ºC for 12.0 h and then backfilled with N_2. N_2 isotherms were generated by incremental exposure to ultra high purity nitrogen up to 1.0 atm in a liquid nitrogen bath (77.0 K), and surface parameters were determined using BET adsorption models included in the instrument SPNtware (BELSORP-Max).

General procedure:

1. Organogel preperation:

The mixture of host **P5N** (5.0 mg) and guest **G** (5.0 mg) were added into cyclohexanol (0.2 mL), the mixture was heated dissolve, then cooled to room temperature, obtaining stable gel (organogel, yellow).

2. Xerogel preparation:

The organogel was heated to dissolve, then it was dumped on the clear glass plate and aired at room temperature, obtaining the xerogel.

3. ^{1}H NMR experiment:

(1). The host (P5N)-guest (G) ^{1}H NMR titration:

The **P5N** (5 mg, 3.17×10^{-6} mol) was dissolved in the DMSO-d_6 (0.5 mL), then a series of different equivalents of **G** (i.e. 0.2 equiv., 0.5 equiv., 1.0 equiv., 1.5 equiv., 2.0 equiv., 2.5 equiv., 3.0 equiv.,) were added into the solution of **P5N** and recorded their ^{1}H NMR, respectively.

(2). The concentrations-dependent ^{1}H NMR of P5N:

A serious of DMSO-d_6 solutions of **P5N** with different concentrations ((a) 1.0 mM; (b) 2.0 mM; (c) 5.0 mM; (d) 10.0 mM; (e) 15.0 mM; (f) 20.0 mM; (g) 30.0 mM) were prepared. Then record their ^{1}H NMR, respectively.

(3). The host (SPN-TDPG)-guest (Hg^{2+}) ^{1}H NMR titration:

The xerogel of the **SPN-TDPG** (5 mg) was dissolved in the DMSO-d_6 (0.5 mL), then different equivalents (0 equiv.; 0.2 equiv.; 0.5 equiv.; 1.0 equiv.; 1.5 equiv) of Hg^{2+} (0.1 M, in DMSO-d_6) were added into the DMSO-d_6 solutions of the **SPN-TDPG** and record their ^{1}H NMR, respectively.

(4). The host (SPN-TDPG-Hg)-guest (Br^-) ^{1}H NMR titration:

The xerogel of the **SPN-TDPG-Hg** (5 mg) was dissolved in the DMSO-d_6 (0.5 mL), then different equivalents (0 equiv.; 0.2 equiv.; 0.5 equiv.; 1.0 equiv.; 1.5 equiv) of Br^- (0.1 M, in DMSO-d_6) were added into the DMSO-d_6 solutions of the **SPN-TDPG** and record their ^{1}H NMR, respectively.

4. Fluorescence titration:

(1). Fluorescence titration based on different concentrations cations:

A serious of the **SPN-TDPG** gels with different concentrations (0.05 equiv., 0.1 equiv., 0.15 equiv., 0.2 equiv., and so on) metal ions (Fe^{3+} and Hg^{2+}) were prepared by dissolving **P5N** (5 mg), **G** (5 mg)

and proper equivalent of metal salt in cyclohexanol (0.25 mL). Then record their fluorescence intensity at 528 nm wavelength.

(2). Fluorescence titration based on different equivalent anions:

The metal-**SPN-TDPG** (**SPN-TDPG-Fe** or **SPN-TDPG-Hg**) gels with different equivalents (0.1 equiv., 0.2 equiv., 0.3 equiv., 0.4 equiv., 0.5 equiv. and so on) of anions (F^- or Br^-) were prepared by dissolve **SPN-TDPG**, metal ions and proper equivalent of anions salt in cyclohexanol (0.2 mL). Then record their fluorescence intensity at the 528nm wavelength and the limit of detection (LOD) calculated on the basis of 3σ/m method.

5. Pollutant removal experiments:

We performed the experiments of pollutant removal at room temperature (25.0 ºC) in water. Firstly, 0.0025 g **SPN-TDPG** xerogel was transferred to a 5.0 mL glass sample bottle. A pollutant stock solution (10 μM, 5.0 mL) was added to the glass sample bottle. The mixture was stirred and the suspension in the bottle (1.00 mL) was taken by a syringe at different intervals and then filtered immediately by using a LABMAX 0.2 μm membrane filter. UV–*vis* spectroscopy was used to determine the residual concentration of the pollutants in each sample.

6. Water regain analysis:

Water regain is an important property of the materials for water treatment. **SPN-TDPG** was dispersed in deionized water for 1.00 hour and then the wet **SPN-TDPG** was filtered by using filter paper. The polymer was collected and blotted by using additional filter paper, and then weighed. These experiments were carried out with three replicates to find the average as the water regain of the **SPN-TDPG**. The water regain of **SPN-TDPG**, which is expressed as the weight percent, was determined from the average of three measurements.

*Synthesis of compound **L**, **P5**.*

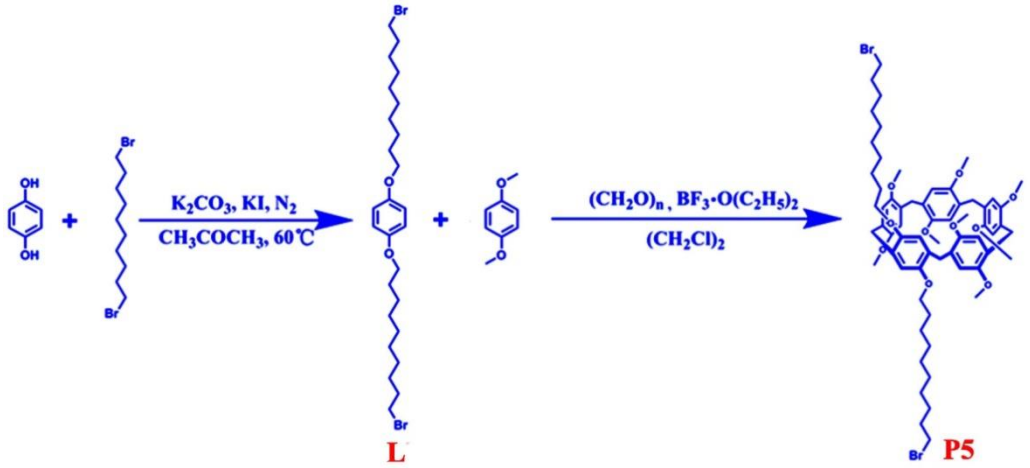

The mixture of 1,10-dibromodecane (1.20 g, 4.0 mmol) and KI (0.66 g, 4.0 mmol) was added to a solution of K_2CO_3 (0.14 g, 1.0 mmol) and hydroquinone (0.11 g, 1.0 mmol) in acetone (200 mL). The mixture was heated under nitrogen atmosphere at reflux for 72 h. The solid was filtered and the solvent was removed. The residue was recrystallized in dichloromethane and petroleum ethers. The product **L** was collected by filtration, and dried under vacuum (0.45 g, 82 %). Mp: 83-85 °C. The ^{1}H NMR spectrum of **L** is shown in FigureS1. ^{1}H NMR (600 MHz, $CDCl_3$). δ 6.81 (s, 4H), 3.89 (t, *J* = 4.4 Hz, 4H) , 3.40 (t, *J* = 4.4 Hz, 4H), 1.87–1.82 (m, 4H), 1.77–1.72 (m, 4H), 1.46–1.30 (m, 24H).

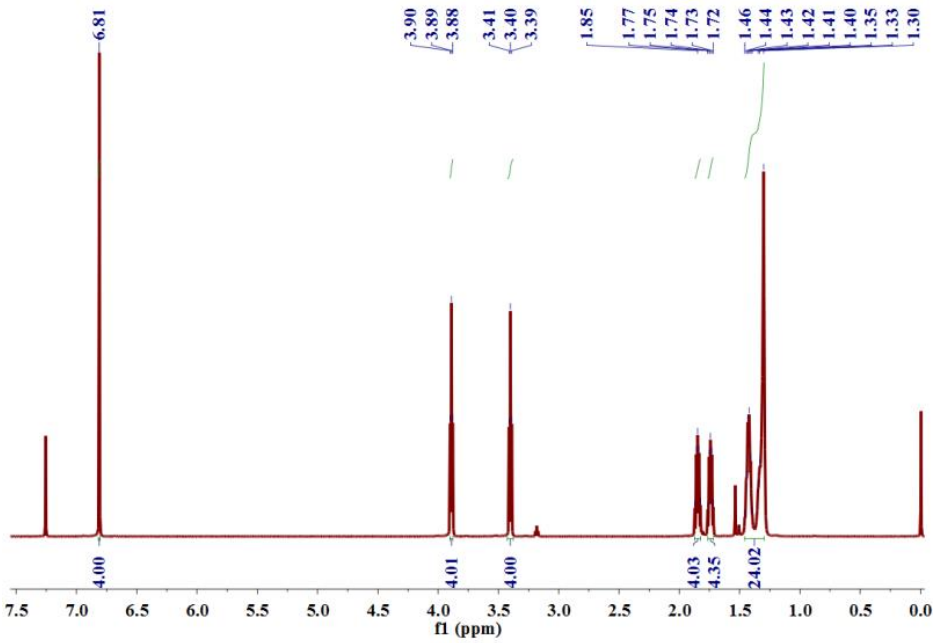

Figure S1. ^{1}H NMR spectrum of compound **L** ($CDCl_3$, 600 MHz, 298 K).

To a solution of 1,4-dimethoxybenzene (3.36 g, 24.0 mmol) and L (1.60 g, 3.0 mmol) in 1,2-dichloroethane (200 mL) was added paraformaldehyde (0.75 g, 25.0 mmol). Then, boron

trifluoride diethyl etherate ($BF_3O(C_2H_5)_2$, 4.5 ml) was added to the solution, and the mixture was stirred at 30 °C for 15-30 min. The solution was poured into water (100 mL) to quench the reaction. The mixture was filtered and the solvent was removed. The residue was dissolved in dichloromethane. The organic layer was dried over anhydrous Na_2SO_4 and evaporated to afford the crude product, which was isolated by column chromatography using ethyl acetate/petroleum ether (v/v, 1:40) to give **P5** as a white solid (1.39 g, 40 %). Mp: 111-113 °C. The proton NMR spectrum of **P5** is shown in FigureS2. ^{1}H NMR (600 MHz, $CDCl_3$) δ (ppm): 6.95-6.86 (m, 10H), 3.94 (t, J = 4.4 Hz, 4H), 3.79 (s, 10H), 3.77-3.76 (m, 28H), 1.87-1.82 (m, 6H), 1.54-1.50 (m, 7H), 1.33 (m, 7H), 1.17 (s, 6H), 0.88-0.86 (m, 6H). The 13C NMR spectrum of **P5** is shown in FigureS3. ^{13}C NMR (150 MHz, $CDCl_3$) δ (ppm): 150.27, 150.19, 150.16, 149.51, 128.10, 128.07, 127.95, 114.06, 113.47, 113.03, 112.98, 112.93, 67.86, 55.46, 55.25, 55.21, 33.85, 32.16, 29.21, 29.09, 28.07, 27.73. ESI-MS is shown in FigureS4: m/z $[M + NH_4]^+$ calcd. for $C_{63}H_{88}Br_2NO_{10}$ 1178.4769, found 1178.4758.

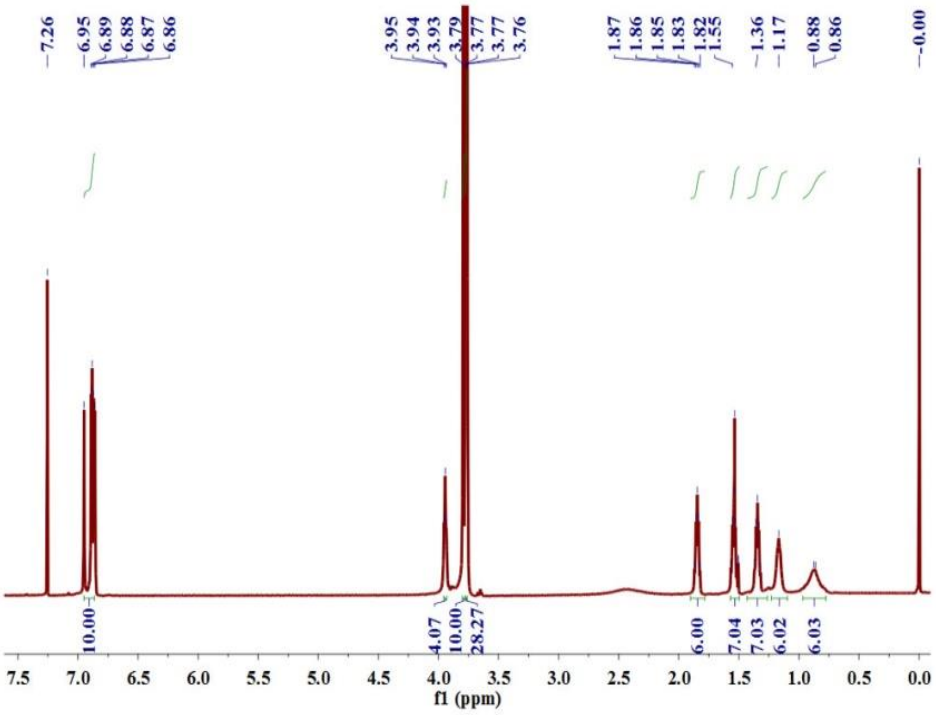

Figure S2. ^{1}H NMR spectrum of compound **P5** ($CDCl_3$, 600 MHz, 298 K).

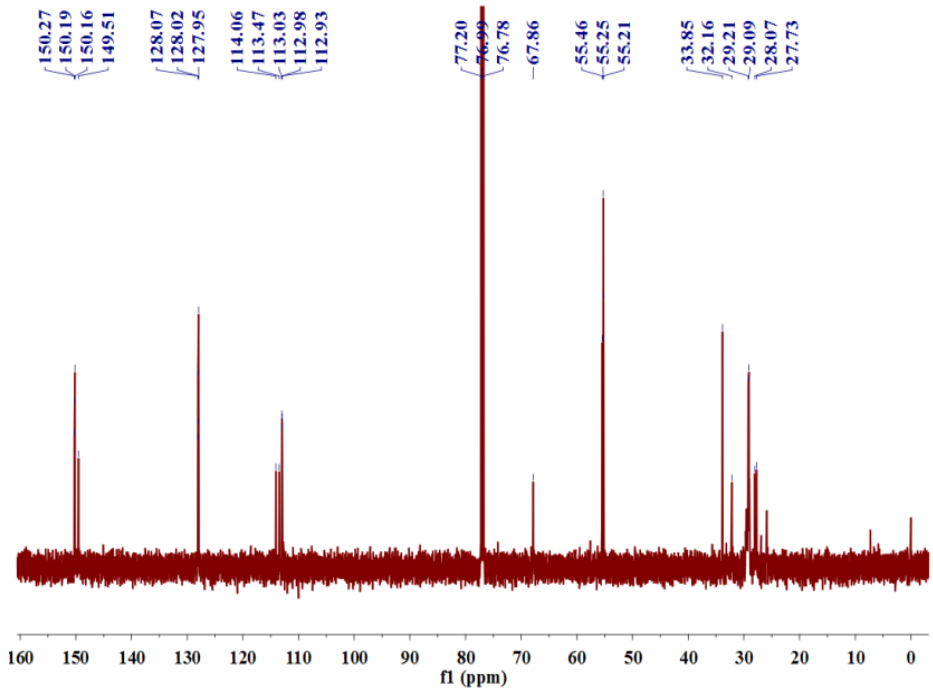

Figure S3. ^{13}C NMR spectrum of compound **P5** ($CDCl_3$, 150 MHz, 298 K).

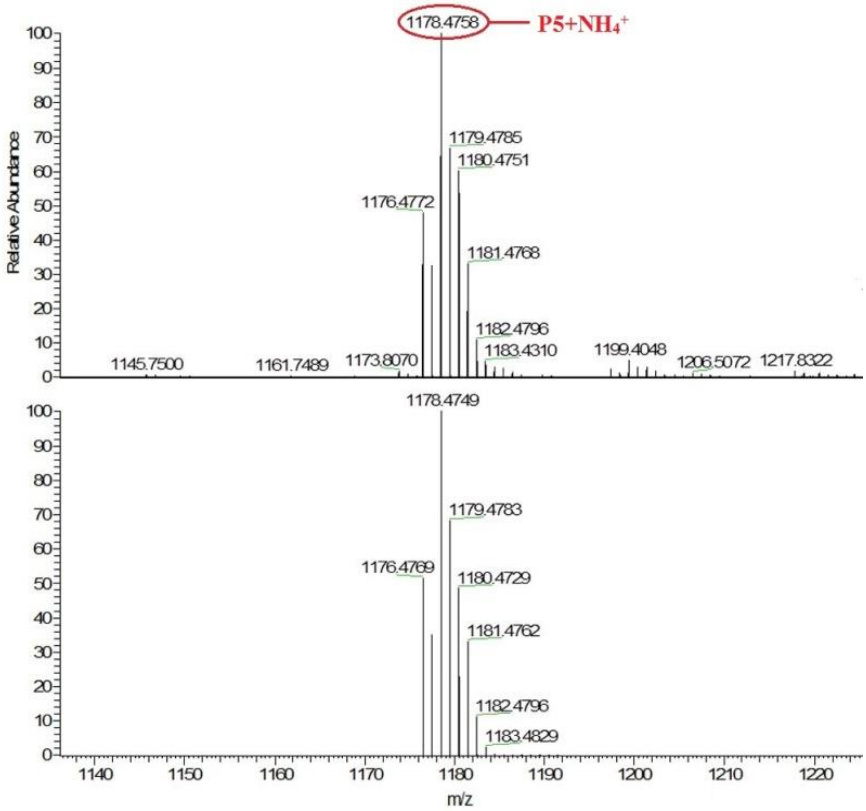

Figure S4. Mass spectrum of **P5.**

*Synthesis of **NM**:*

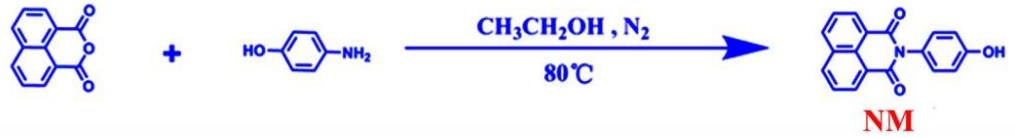

1,8-naphthalic anhydride (0.19 g, 1.0 mmol) was added to a mixture of 4-aminophenol (0.22 g, 2.0 mmol) in C_2H_5OH (60 mL), and the reaction mixture was stirred reflux 48 h. After reaction was finished, the solvent was filtered under reduced pressure. The crude product was elution with ethanol afforded **NM** as a white solid (0.28 g, 96 %). Mp: > 290 °C. The proton NMR spectrum of **NM** is shown in FigureS5. ^{1}H NMR (600 MHz, DMSO-d_6) δ (ppm): 9.63 (s, 1H), 8.45-8.44 (t, J = 5.2 Hz, 4H), 7.85 (t, J = 5.2 Hz, 2H), 7.13-7.11 (d, J = 5.6 Hz, 2H), 6.86-6.85 (d, J = 5.6 Hz, 2H). The ^{13}C NMR spectrum of **NM** is shown in FigureS6. ^{13}C NMR (150 MHz, DMSO-d_6) δ (ppm): 164.28, 157.55, 134.72, 130.34, 127.32, 123.07, 115.82.

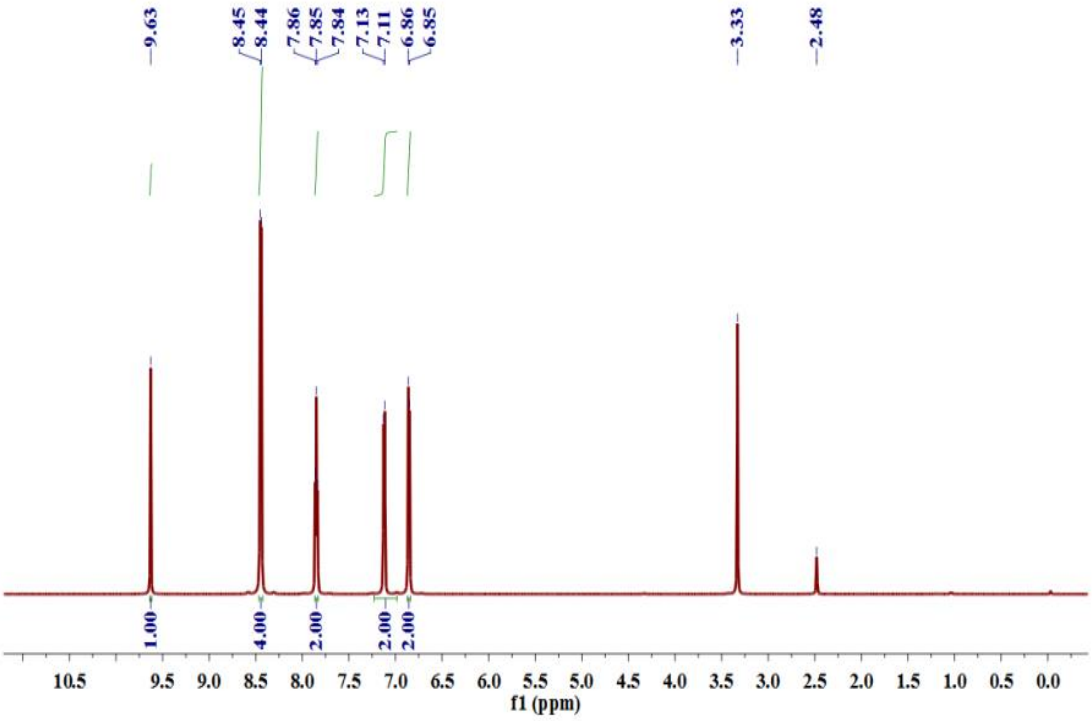

Figure S5. ^{1}H NMR spectrum of compound **NM** (DMSO–d_6, 600 MHz, 298 K).

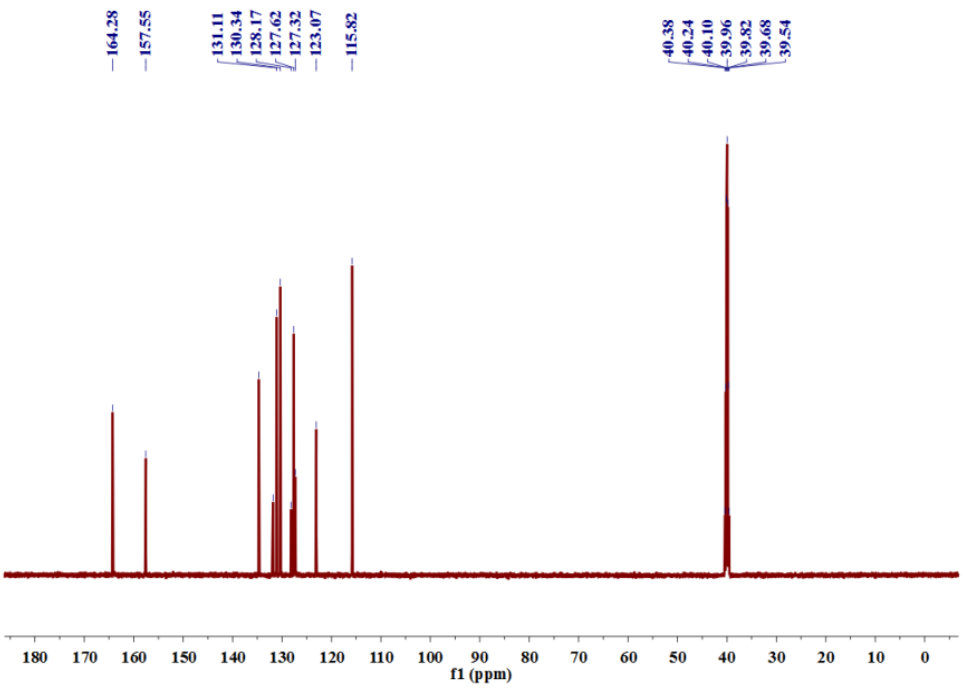

Figure S6. ^{13}C NMR spectrum of compound **NM** (DMSO–d_6, 150 MHz, 298 K).

*Synthesis of **P5N**:*

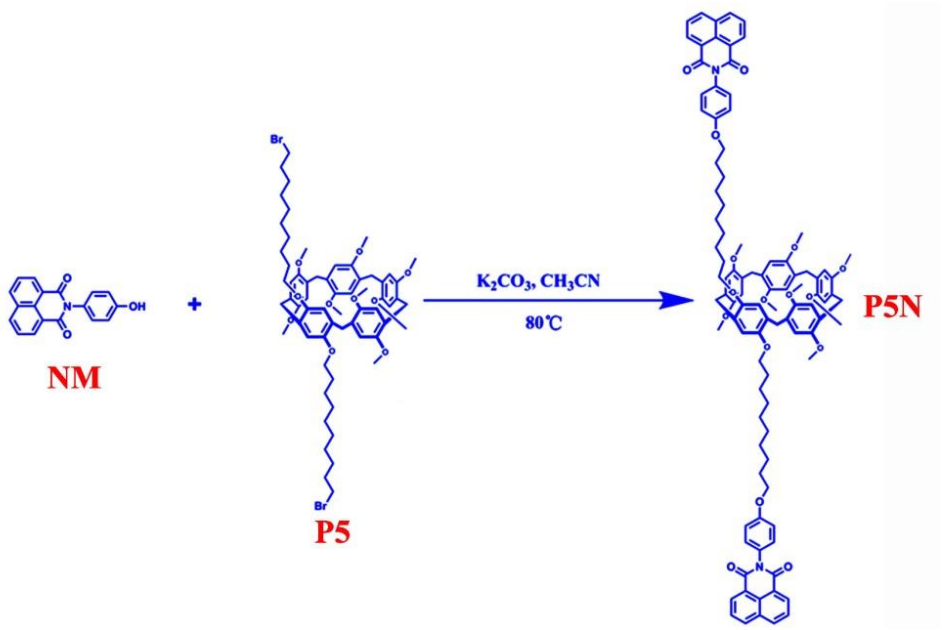

Compound **P5** (1.16 g, 1.0 mmol) was added to a mixture of compound **NM** (0.87 g, 3.0 mmol), and K_2CO_3 (0.42 g, 3.0 mmol) in acetonitrile (50 mL), and the resulting mixture was stirred for 48 h. After reaction was finished, the solvent was evaporated under reduced pressure. The crude product was purified by chromatography on silica gel. Elution with a mixture of dichloromethane/ethyl acetate (v/v, 50:1) afforded **P5N** as a yellow solid (1.29 g, 82 %). Mp: 102-103 °C. The proton NMR spectrum of **P5N** is shown in FigureS7. ^{1}H NMR (600 MHz, $CDCl_3$) δ (ppm): 8.65 (d, J = 7.2

Hz, 4H), 8.27-8.26 (d, J = 7.2 Hz, 4H), 7.79 (t, J = 7.6 Hz, 4H), 7.22-7.21 (d, J = 8.7 Hz, 4H), 7.03-7.02 (d, J = 8.7 Hz, 4H), 6.87-6.80 (m, 10H), 3.91-3.86 (m, 8H), 3.82-3.72 (m, 10H), 3.72-3.69 (m, 24H), 1.82-1.76 (m, 3H), 1.54-1.21 (m, 19H), 1.05 (s, 3H),0.89-0.85 (m, 7H). The ^{13}C NMR spectrum of **P5N** is shown in FigureS8. ^{13}C NMR (150 MHz, $CDCl_3$) δ (ppm): 164.56, 159.20, 150.65, 134.16, 131.73, 131.55, 129.43, 128.10, 126.99, 122.91, 115.11, 68.29, 55.71, 55.68, 55.55, 29.08, 29.03. ESI-MS is shown in FigureS9: m/z $[M]^+$ calcd. for $C_{99}H_{104}N_2O_{16}$ 1577.7419, found 1577.7498.

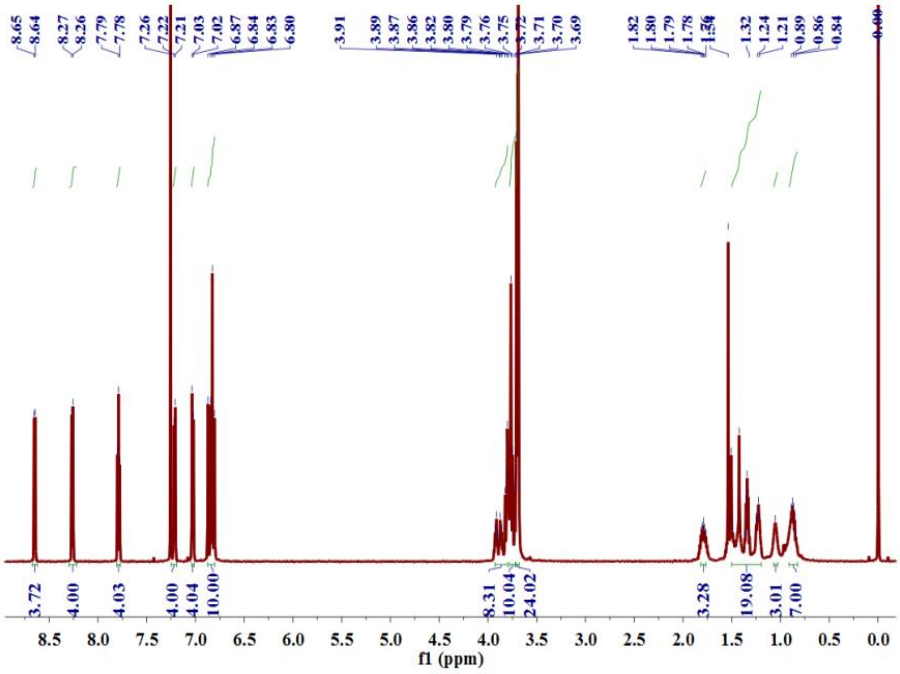

Figure S7. ^{1}H NMR spectrum of compound **P5N** ($CDCl_3$, 600 MHz, 298 K).

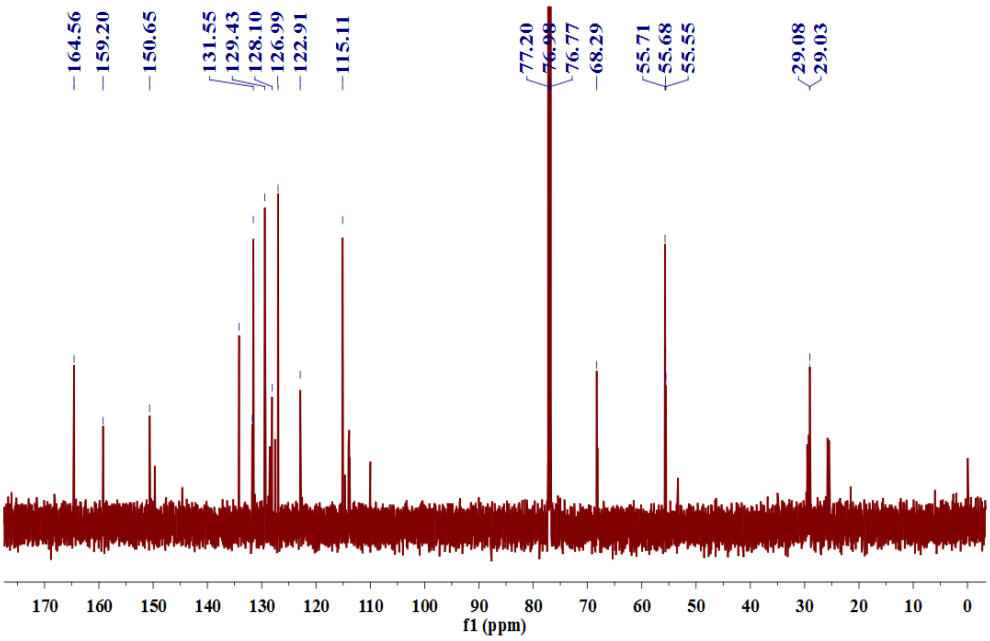

Figure S8. ^{13}C NMR spectrum of compound **P5N** ($CDCl_3$, 150 MHz, 298 K).

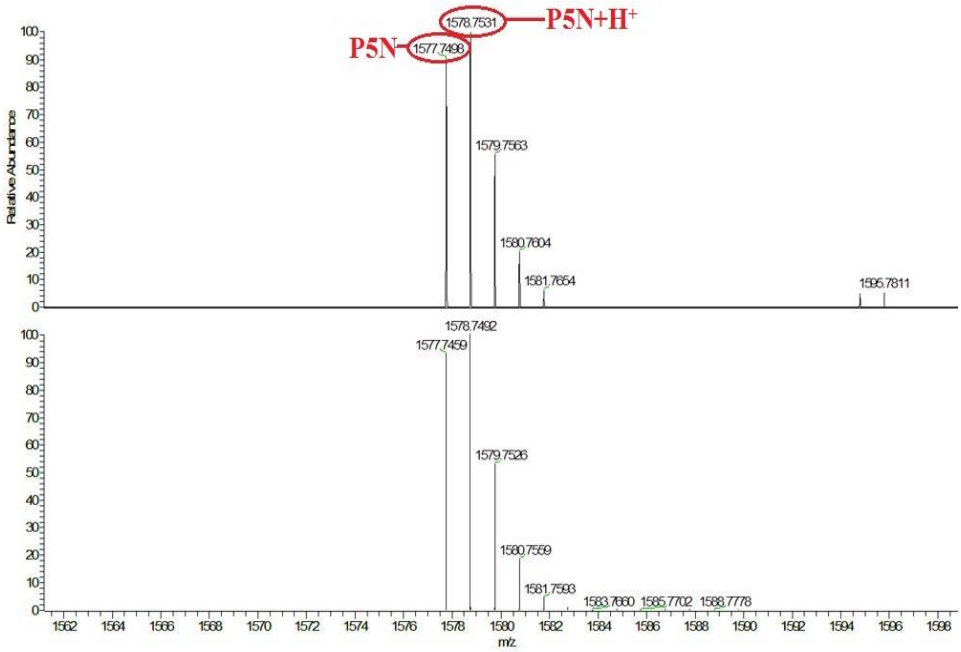

Figure S9. Mass spectrum of **P5N**.

*Synthesis of compound **G**:*

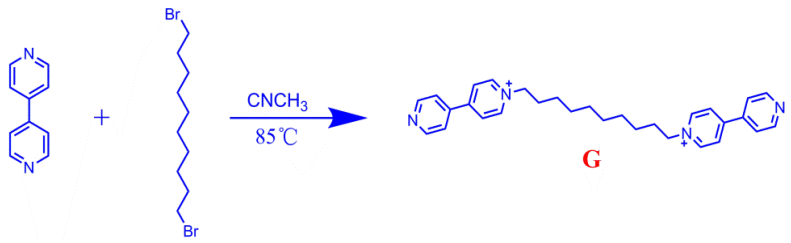

A solution of 1,10-dibromodecane (1.89 g, 6.3 mmol) in CH_3CN (25 mL) was added dropwise into a stirred solution of 4,4'-bipyridine (5.56 g, 35.7 mmol) in CH_3CN (50 mL) and refluxed over night. After it cooled, the suspension was filtered. The solid was washed with CH_3CN and then dried in an oven to afford a pale green solid **G** (3.3 g, 86%). ^{1}H NMR (400 MHz, DMSO-d_6) δ 9.37 (d, *J*=6.7Hz, 4H), 8.89 (d, *J*=6.7Hz, 4H), 8.71 (d, *J*=6.7Hz, 4H), 8.10 (d, *J*=6.1Hz, 4H), 4.72 (t, *J*=7.3Hz, 4H), 1.97(s, 4H), 1.32 (d, *J*=15.5Hz, 12H).

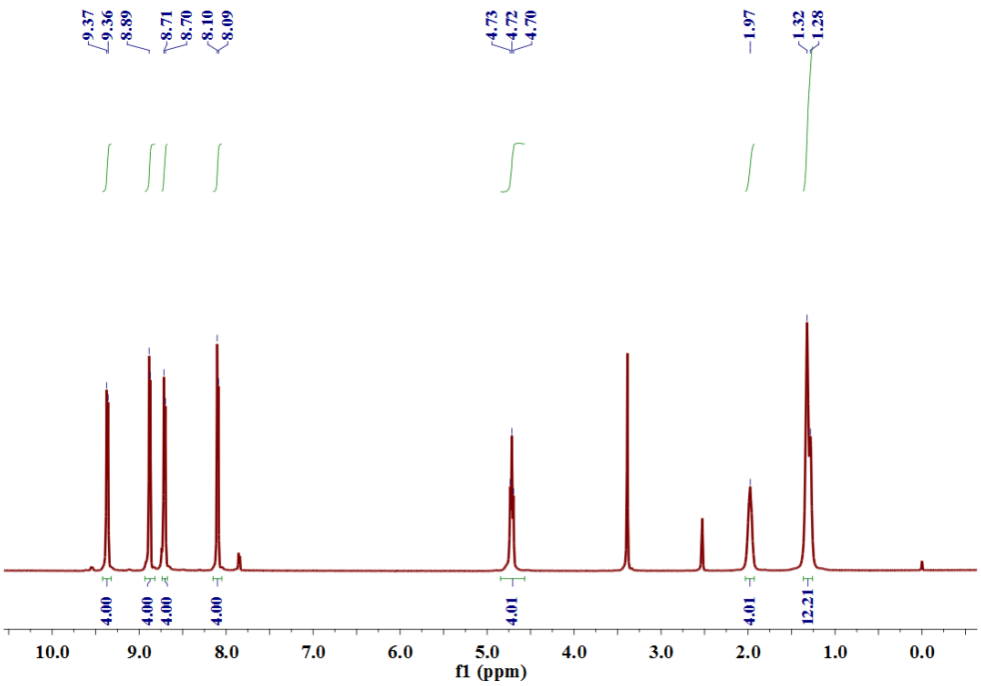

Figure S10. ^{1}H NMR spectrum of **G** (DMSO-d_6, 600 MHz, 298 K).

Table S1. Gelation property of **SPN-TDPG**.

Entry	Solvent	State	CGC (%)	T_{gel}(°C, wt%)
1	Ethyl acetate	S	\	\
2	Ethyl alcohol	P	\	\
3	CCl_4	P	\	\
4	PEG-400	P	\	\
5	Isopropyl alcohol	P	\	\
6	Ethylene glycol	P	\	\
7	Acetone	P	\	\
8	DMF	S	\	\
9	DMF/H_2O (V/V=9:1)	G	9.5 %	45~48 °C
10	DMSO	S	\	\
11	DMSO/H_2O (V/V=8:2)	G	10.0 %	61~63 °C
12	n-Propyl Alcohol	P	\	\
13	Methyl alcohol	P	\	\
14	Tert-butyl alcohol	P	\	\
15	Glycerol	P	\	
16	Isoamyl alcohol	P	\	\
17	n-Butyl alcohol	P	\	\
18	Cyclohexanol	G	2.0 %	55~58 °C
19	N-hexanol	G	3.0 %	50~52 °C
19	CH_2Cl_2	P	\	\
20	Tetrahydrofuran	S	\	\
21	Acetic acid	P	\	\
22	n-Butanol	P	\	\
23	Cyclohexane	P	\	\

State： 10 mg/mL = 1 %, G = Gelation, S = Solution, P = Precipitation.

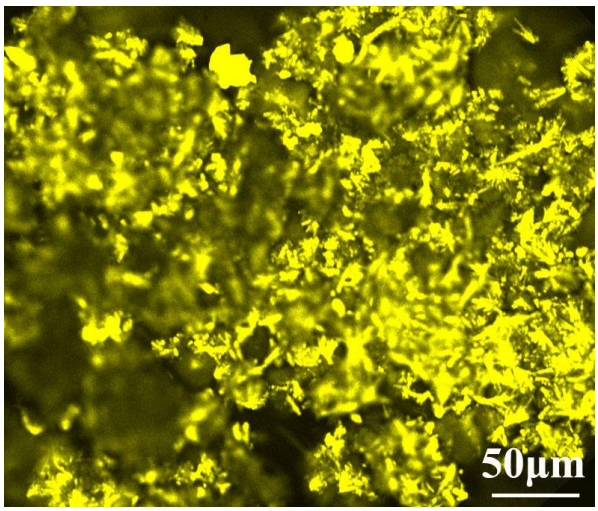

Figure S11. LSCM images of **SPN-TDPG** xerogel.

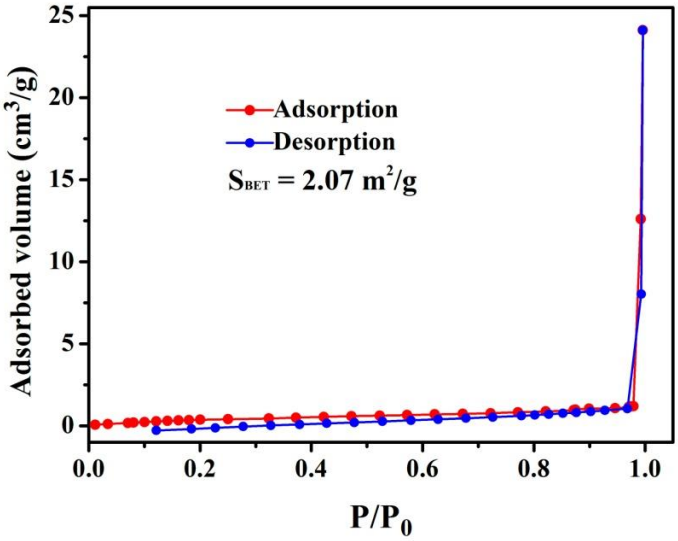

Figure S12. Nitrogen adsorption-desorption isotherm (77.0 K) of **SPN-TDPG**.

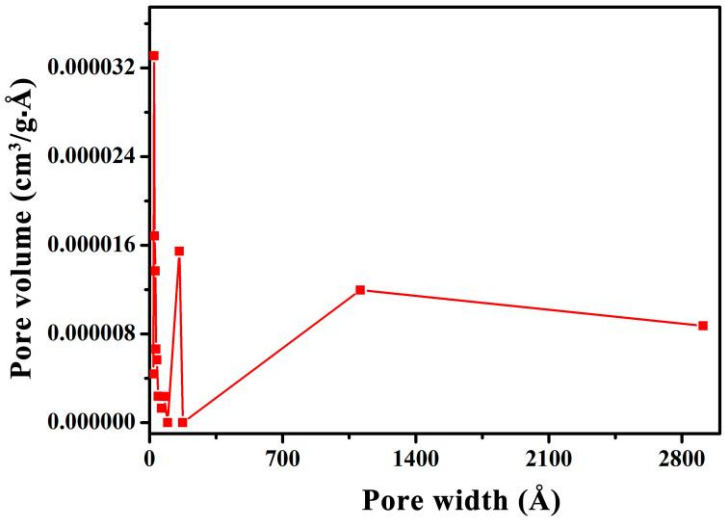

Figure S13 Pore size distribution profiles of **SPN-TDPG.**

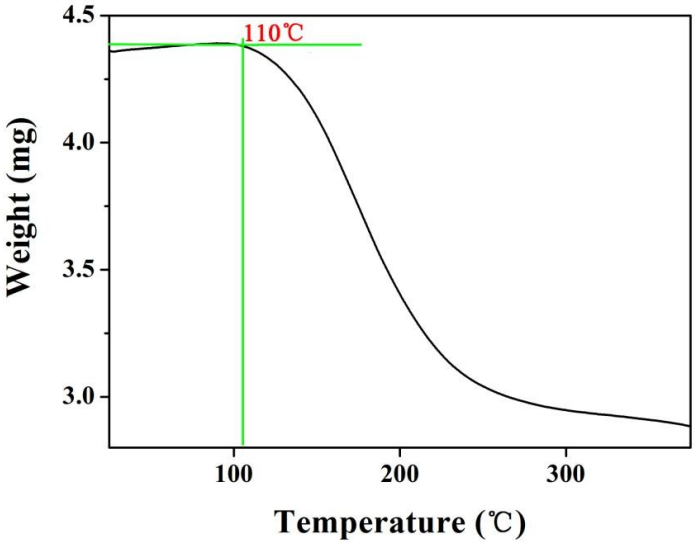

Figure S14. Thermogravimetric analysis of **SPN-TDPG.**

Table S2. Water regain analysis of **SPN-TDPG**. The water regain (expressed as weight percent) of the **SPN-TDPG** was determined from the average (87.4 %) of three measurements.

Entry	M_d(mg)	M_w(mg)	Water regain %
1	30.1	56.3	87.0
2	29.8	55.8	87.2
3	30.6	57.5	87.9

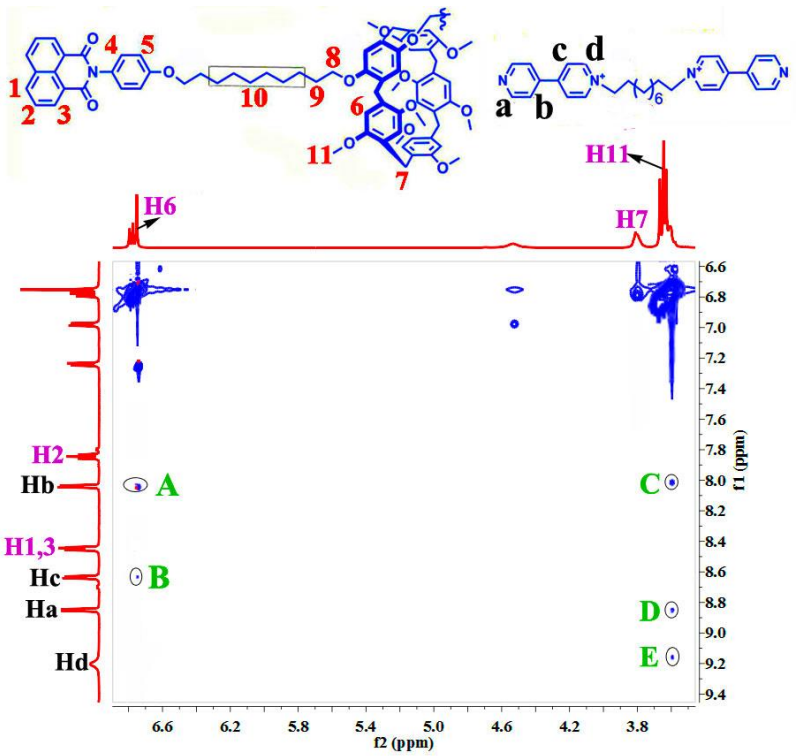

Figure S15. Partial 2D NOESY NMR spectrum of 5.0 mM **P5N** and **G** in DMSO-d_6 solution (600 MHz, 298 K).

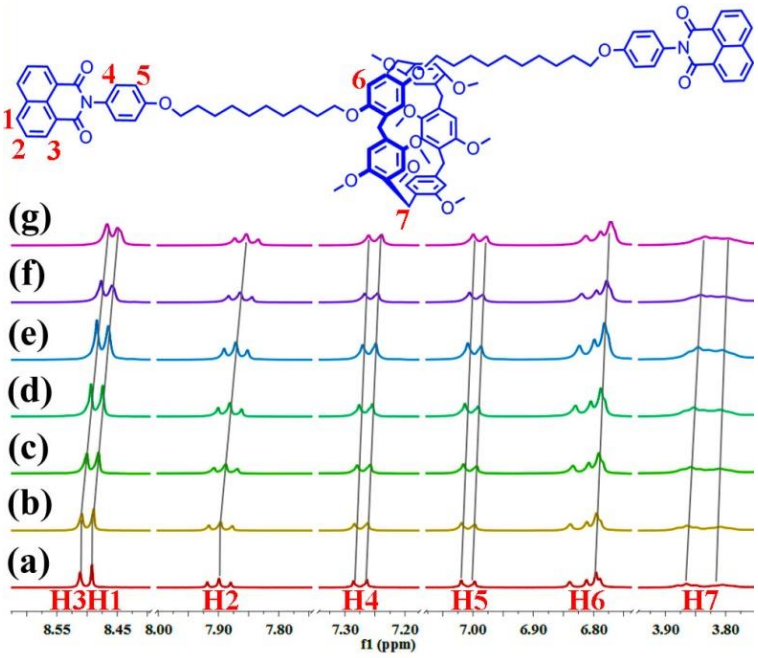

Figure S16. Partial ^{1}H NMR spectra (600MHz, 298 K) of **P5N** in DMSO-d_6 at various concentrations: (a) 1.0 mM; (b) 2.0 mM; (c) 5.0 mM; (d) 10.0 mM; (e) 15.0 mM; (f) 20.0 mM; (g) 30.0 mM.

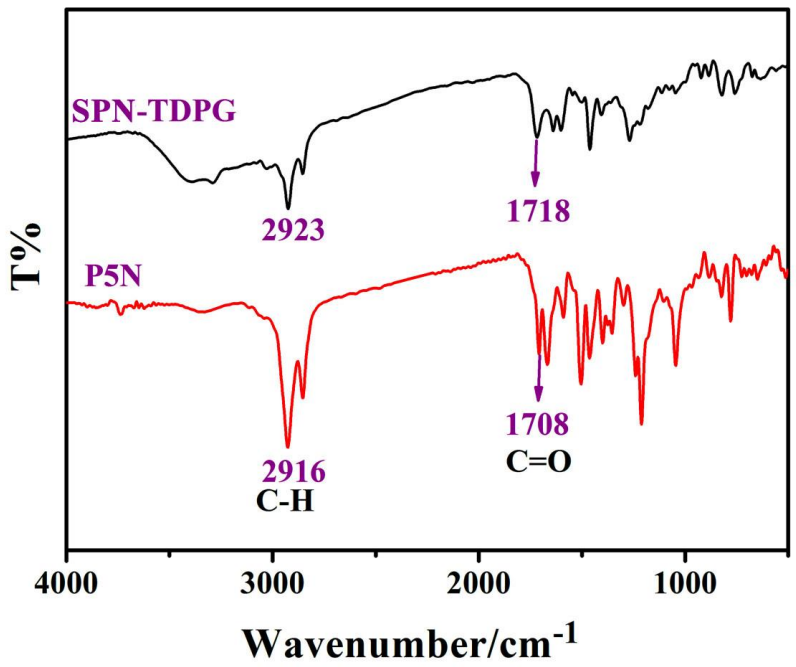

Figure S17. FT-IR spectra of powdered **P5N**, xerogel **SPN-TDPG.**

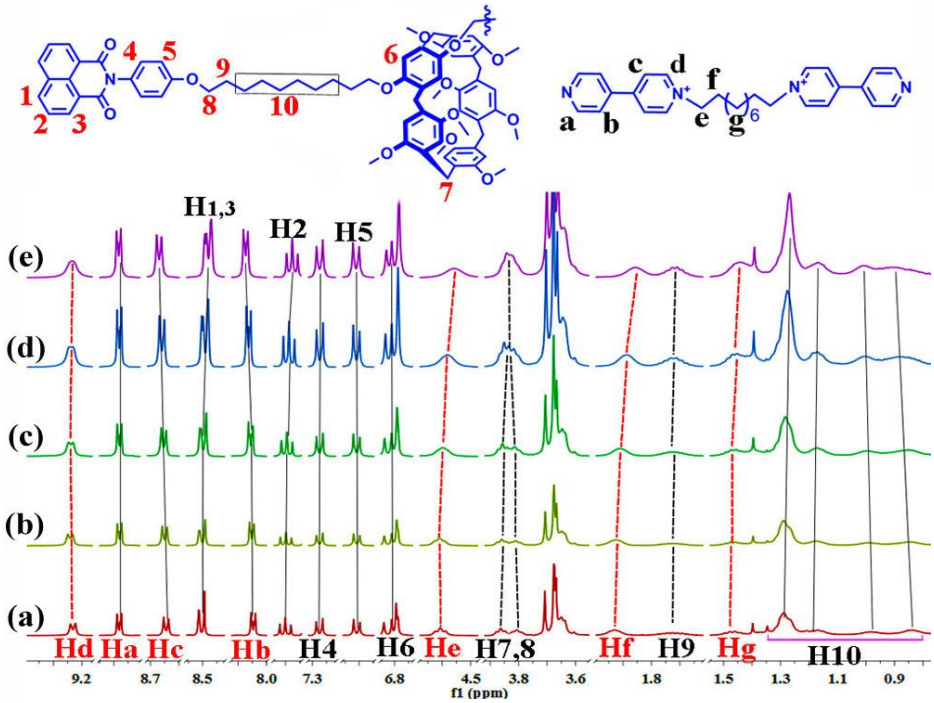

Figure S18. Partial ^{1}H NMR spectra (600 MHz, DMSO-d_6, 298 K) of **P5N** and **G** at different concentrations: (a) 5.0 mM; (b) 10.0 mM; (c) 20.0 mM; (d)40.0 mM; (e) 80.0 mM.

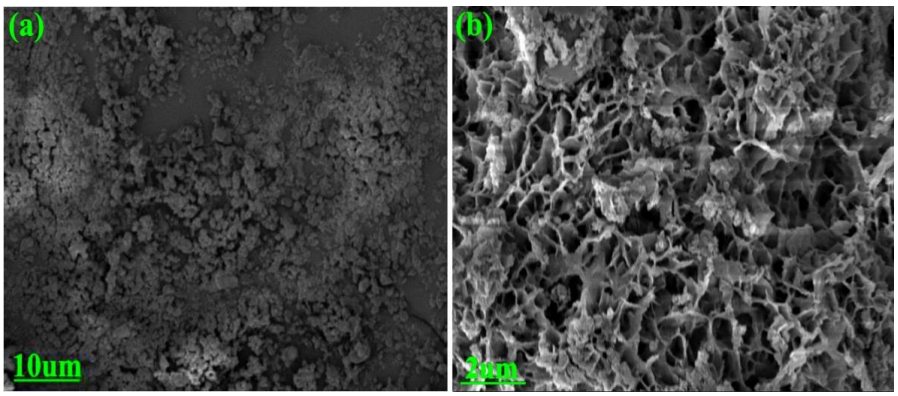

Figure S19. Representative SEM images showing the morphology of (a) **P5N** and (b) **SPN-TDPG**.

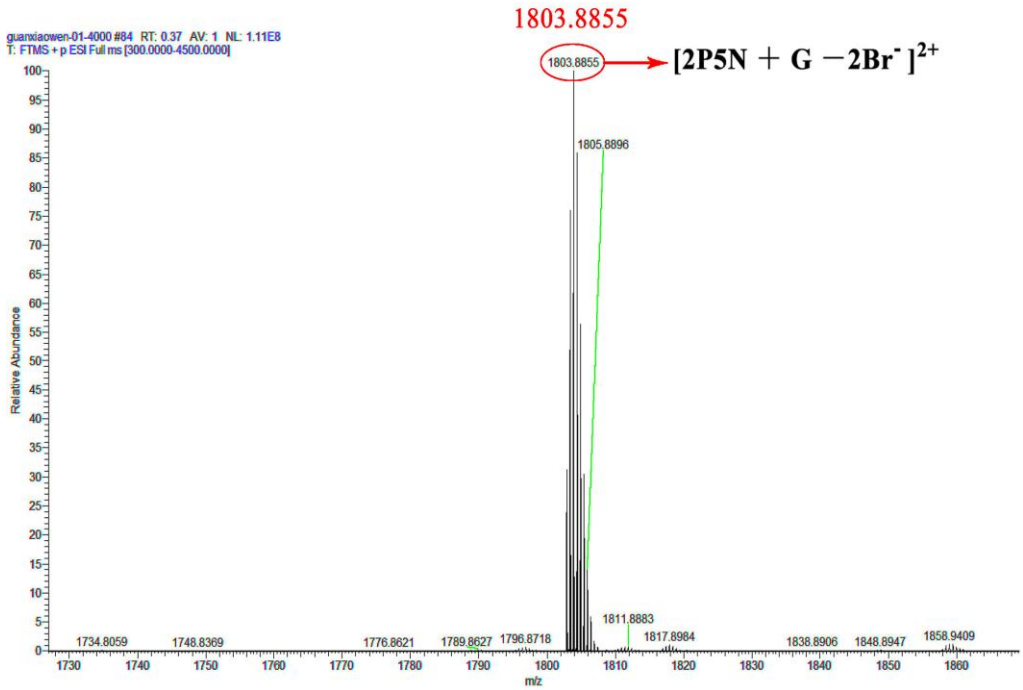

Figure S20. HR-ESI-MS of mixture **P5N** and **G**, clearly indicating the 2:1 stoichiometry for **P5N** and **G**.

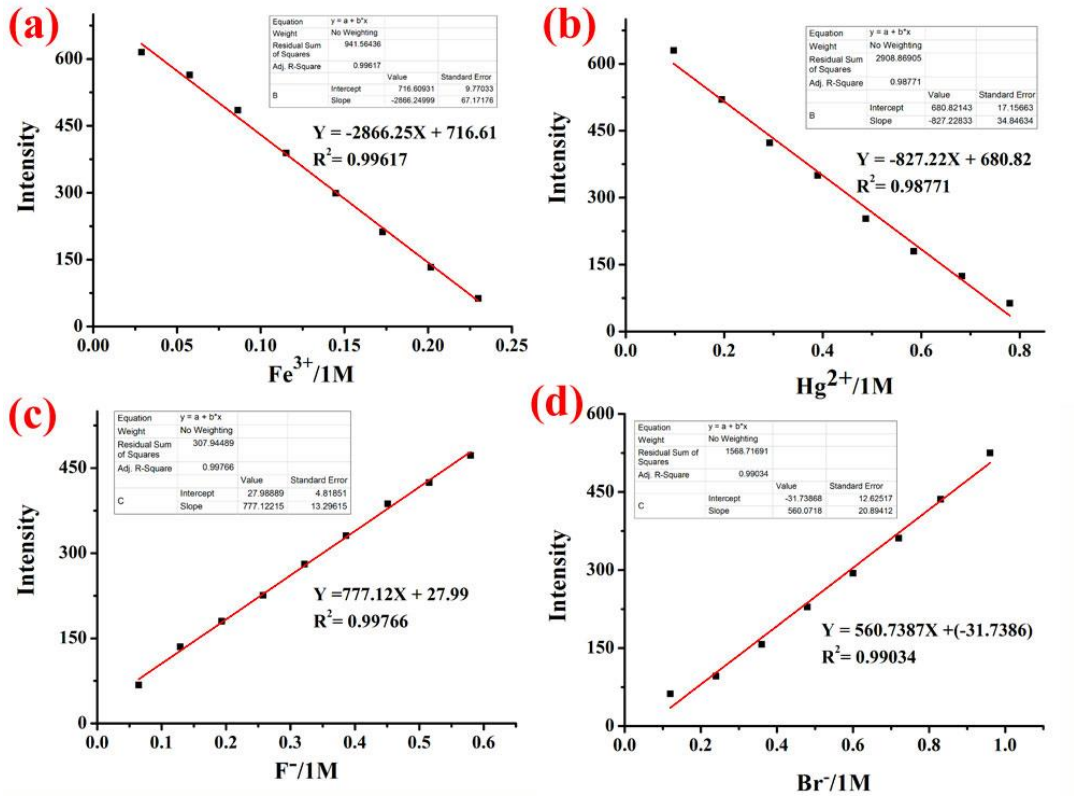

Figure S21. The linear range of (a) **SPN-TDPG** for Fe^{3+}; (b) **SPN-TDPG** for Hg^{2+}; (c) **SPN-TDPG-Fe** for F^-; (d) **SPN-TDPG-Hg** for Br^-.

Table S3. Limits of detection the **SPN-TDPG** or **SPN-TDPG** treated by metal ions for target ions.

Entry	Gel	Target ions	LOD/M
1	SPN-TDPG	Fe^{3+}	9.19×10^{-9}
2	SPN-TDPG	Hg^{2+}	3.95×10^{-8}
3	SPN-TDPG-Fe	F^-	3.38×10^{-8}
4	SPN-TDPG-Hg	Br^-	8.17×10^{-8}

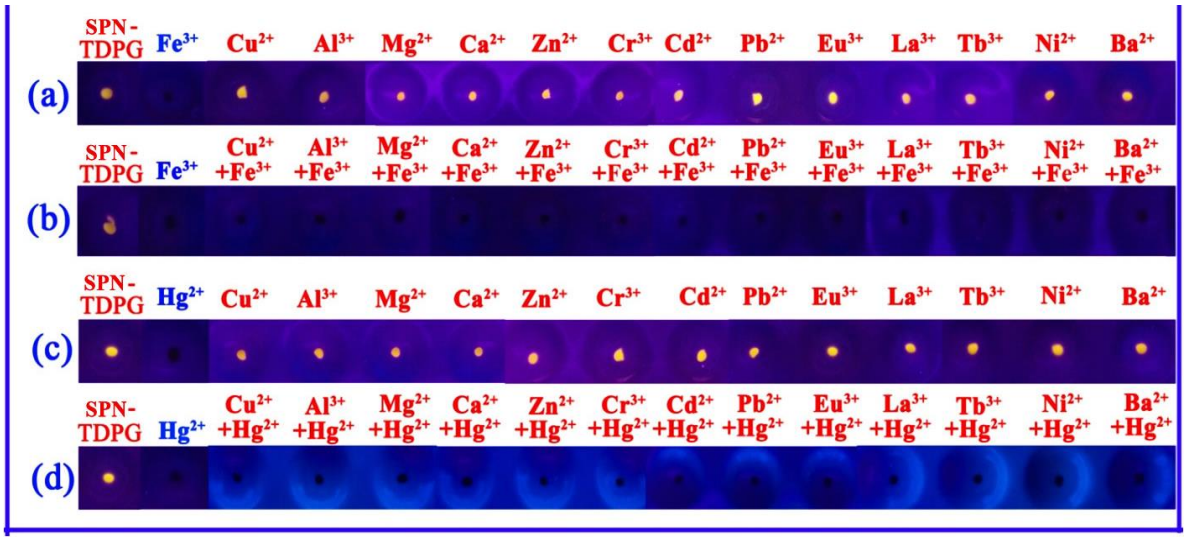

Figure S22. The control experiments: (a) **SPN-TDPG** treated by water solutions of various cations; (b) **SPN-TDPG** contained water solutions of various cations treated by water solution of Fe^{3+}; (c) **SPN-TDPG** treated by water solutions of various cations; (d) **SPN-TDPG** contained water solutions of various cations treated by water solution of Hg^{2+}.

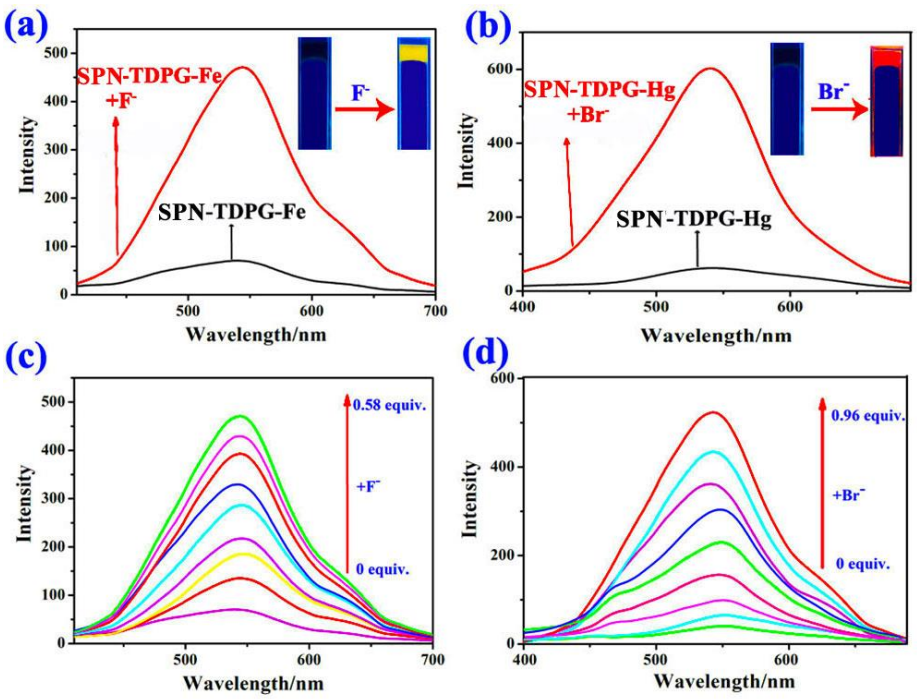

Figure S23. Fluorescence spectra of supramolecular gel (in gelated state) (a) **SPN-TDPG-Fe** and **SPN-TDPG-Fe** + F^-; (b) **SPN-TDPG-Hg** and **SPN-TDPG-Hg** + Br^-; (c) The fluorescent titrations of **SPN-TDPG-Fe** for F^-; (d) The fluorescent titrations of **SPN-TDPG-Hg** for Br^-.

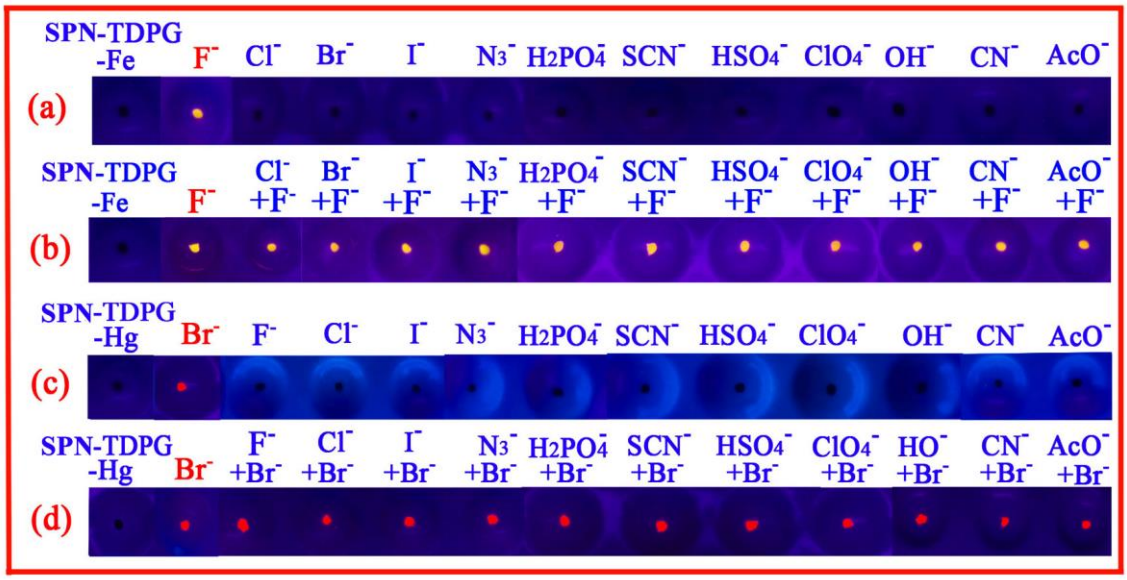

Figure S24. The control experiments: (a) **SPN-TDPG-Fe** and **SPN-TDPG-Fe** treated by water solutions of various anions; (b) **SPN-TDPG-Fe** and **SPN-TDPG-Fe** contained water solutions of various anions treated by water solution of F^-. (c) **SPN-TDPG-Hg** and **SPN-TDPG-Hg** treated by water solutions of various anions; (d) **SPN-TDPG-Hg** and **SPN-TDPG-Hg** contained water solutions of various anions treated by water solution of Br^-.

Table S4. Chemical name, chemical structures and exact weight of pollutants.

Entry	Chemical name	Chemical structures	Molar mass (g/mol)
1	Methylene Blue	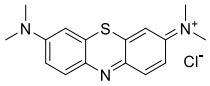	319.09
2	Bismarck Brown Y	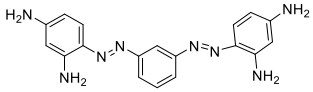	346.16
3	Giemsa's Stain	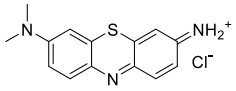	291.06
4	Orangel I	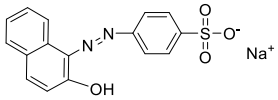	350.03
5	Methyl Orangel	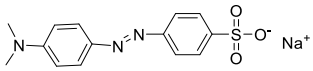	327.06
6	Rhodamine B	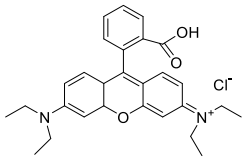	481.03
7	Sudan I	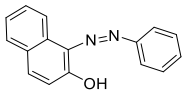	248.28
8	Sudan II	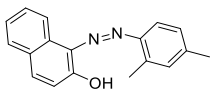	276.33
9	Picric Acid	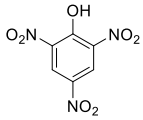	229.10
10	1-Naphthol		144.17
11	Potassium Permanganate	$KMnO_4$	158.03
12	Potassium Dichromate	$K_2Cr_2O_7$	294.18

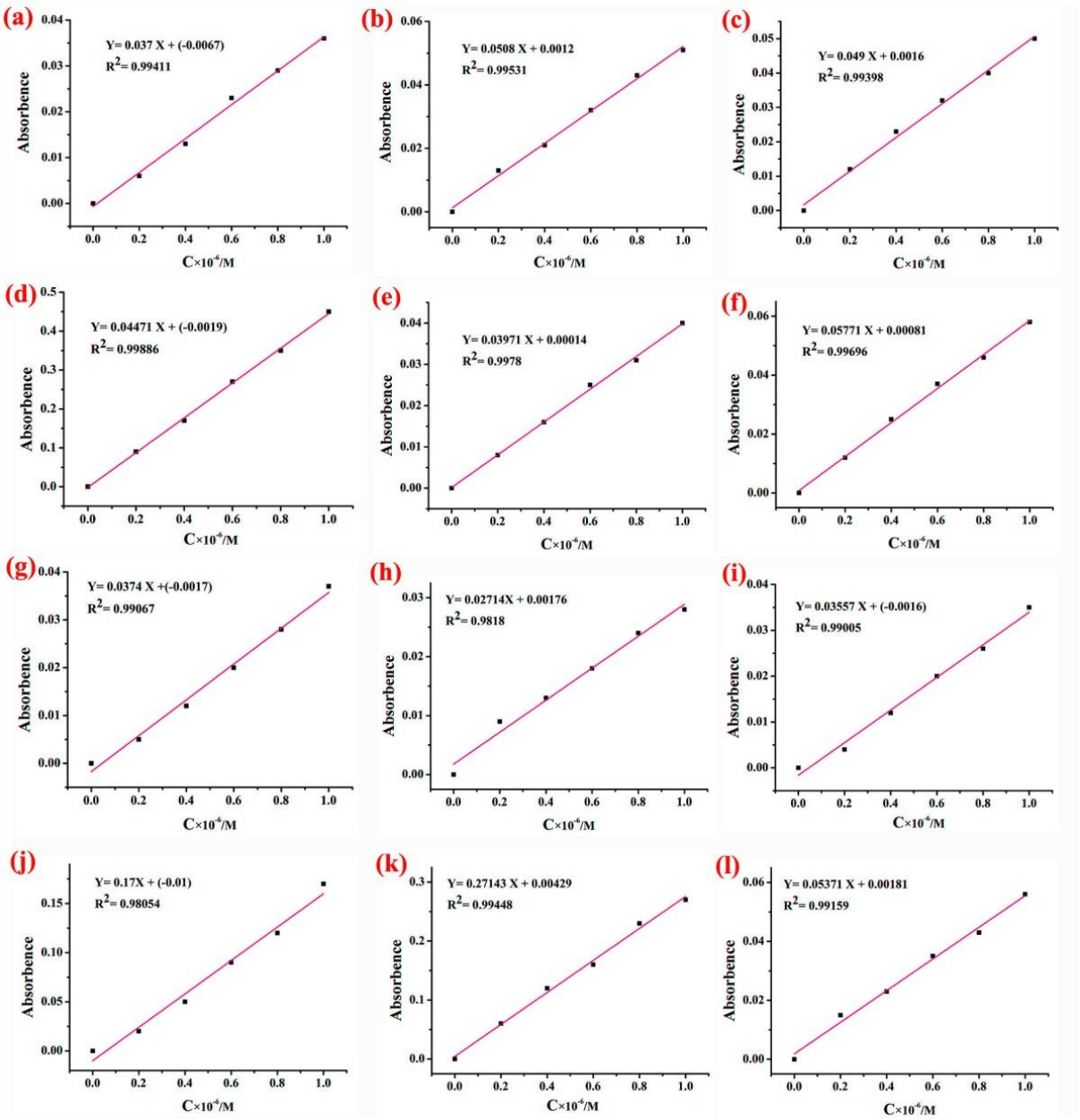

Figure S25. A plot of concentration vs. absorbance intensity is shown. (a) methylene blue; (b) Bismarck brown Y; (c) Giemsa's stain; (d) orangel I; (e) methyl orangel; (f) rhodamine B; (g) Sudan I; (h) Sudan II; (i) picric acid; (j) 1-naphthol; (k) $KMnO_4$; (l) $K_2Cr_2O_7$.

Table S5. The required contact time to reach equilibrium on the pollutants adsorptions. The amount of the adsorbent used in this study is 0.5 mg/mL.

Entry	Pollutants	Equilibrium Time (min)
1	Methylene Blue	20
2	Bismarck Brown Y	20
3	Giemsa's Stain	15
4	Orangel I	20
5	Methyl Orangel	25
6	Rhodamine B	25
7	Sudan I	20
8	Sudan II	25
9	Picric Acid	15
10	1-Naphthol	20
11	$KMnO_4$	5
12	$K_2Cr_2O_7$	10

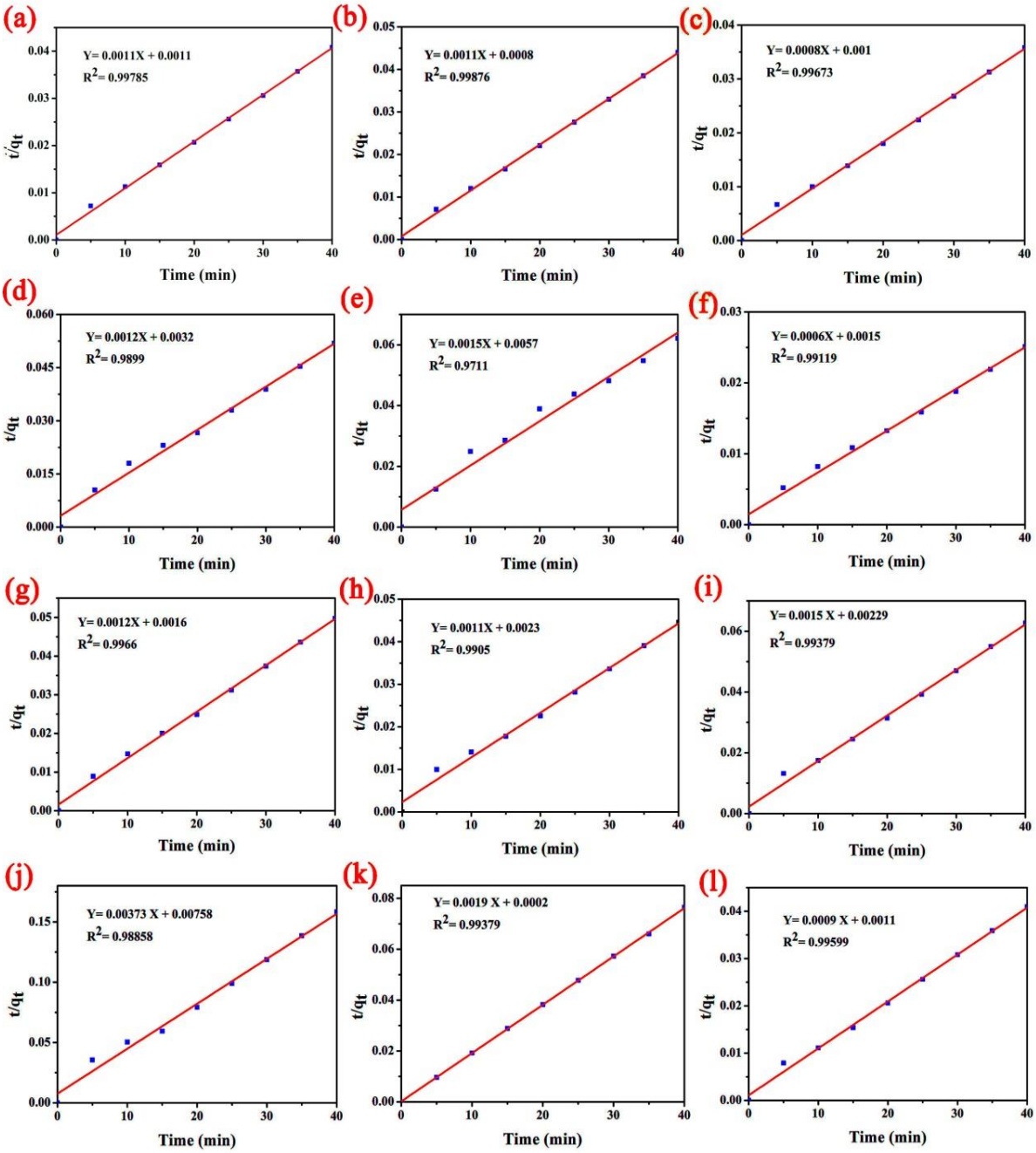

Figure S26. Pseudo-second-order plots for **SPN-TDPG**: (a) methylene blue; (b) Bismarck brown Y; (c) Giemsa's stain; (d) orangel I; (e) methyl orangel; (f) rhodamine B; (g) Sudan I; (h)Sudan II; (i) picric acid; (j) 1-naphthol; (k) $KMnO_4$; (l) $K_2Cr_2O_7$. Here *t* (min) is the contact time of each pollutant solution with **SPN-TDPG** and q_t (mg/mg) is the amount of each pollutant adsorbed per gram of **SPN-TDPG**.

Table S6. Rates of each pollutant uptake by **SPN-TDPG**.

Entry	Pollutants	$k_{obs}\times10^{-3}$ (mg/mg min)	R^2
1	Methylene Blue	1.10	0.99
2	Bismarck Brown Y	1.51	0.99
3	Giemsa's Stain	0.64	0.99
4	Orangel I	0.45	0.99
5	Methyl Orangel	0.39	0.97
6	Rhodamine B	0.24	0.99
7	Sudan I	0.90	0.99
8	Sudan II	0.53	0.99
9	Picric Acid	0.98	0.99
10	1-Naphthol	1.83	0.99
11	$KMnO_4$	18.1	0.99
12	$K_2Cr_2O_7$	0.74	0.99

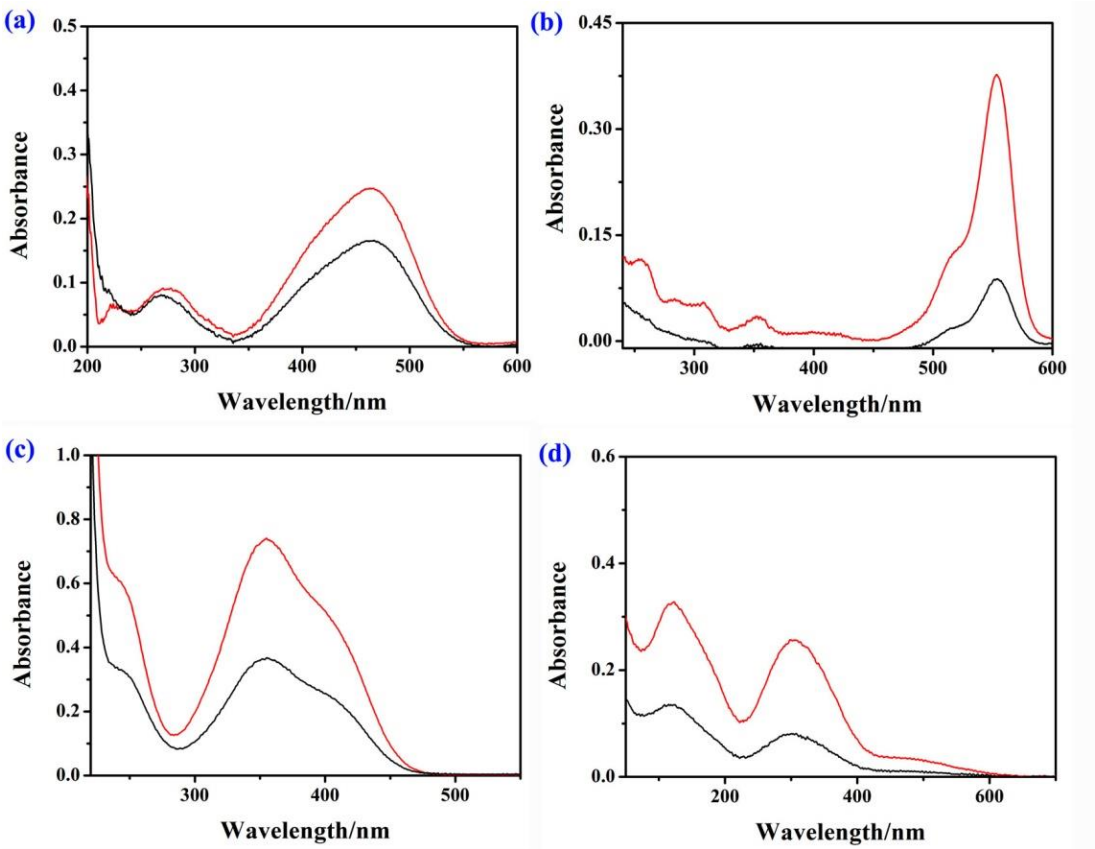

Figure S27. UV–*vis* spectra recorded before (red line)- after (black line, 40min) of adsorption (a) methyl orange, (b) rhodamine B, (c) picric acid and (d) $K_2Cr_2O_7$ with activated carbon (0.5 mg/mL).

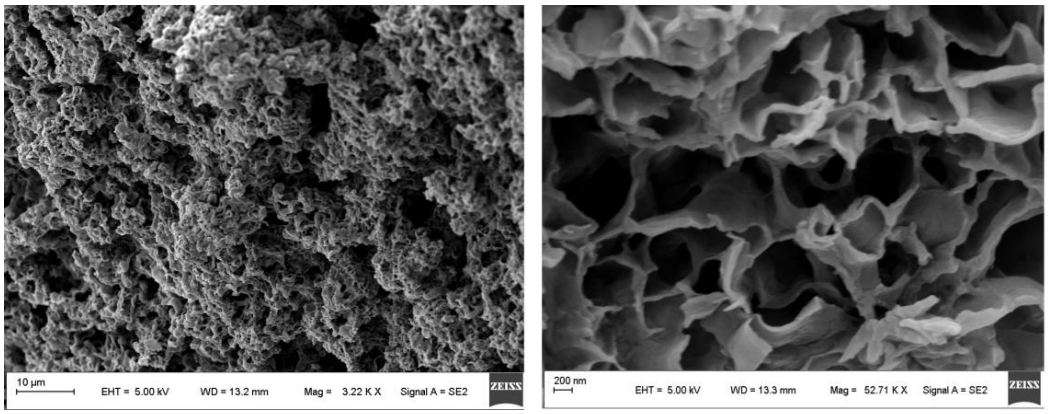

Figure S28. SEM images showing the morphology of regeneration **SPN-TDPG.**

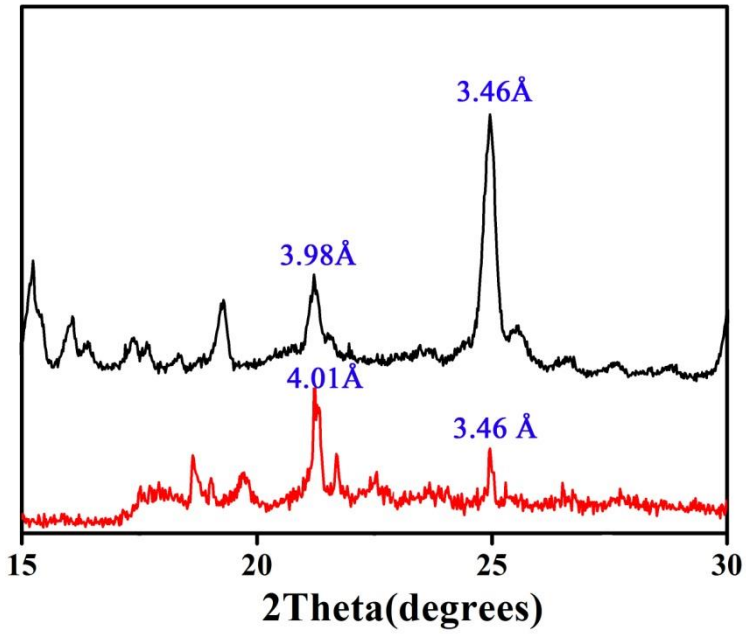

Figure S29. PXRD diagrams of **SPN-TDPG** and regeneration **SPN-TDPG.**

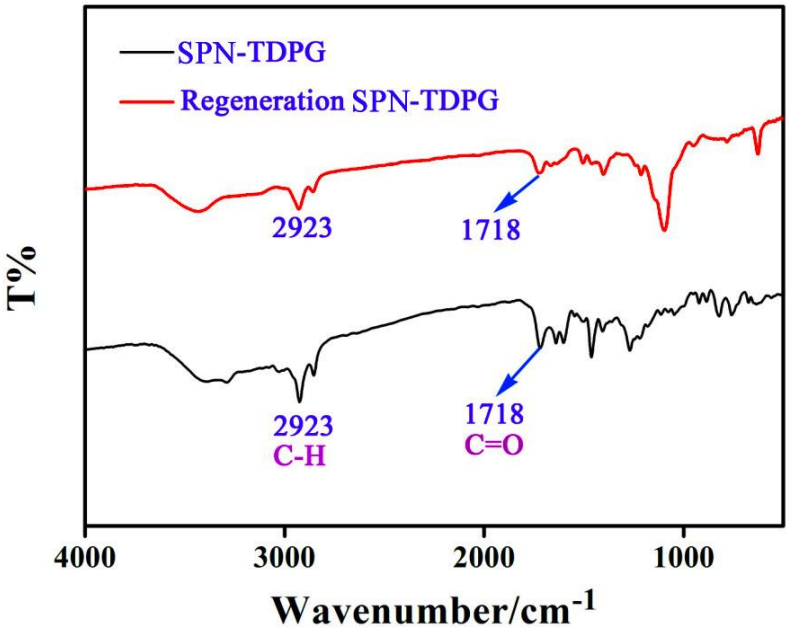

Figure S30. FT-IR spectra of **SPN-TDPG** and regeneration **SPN-TDPG.**

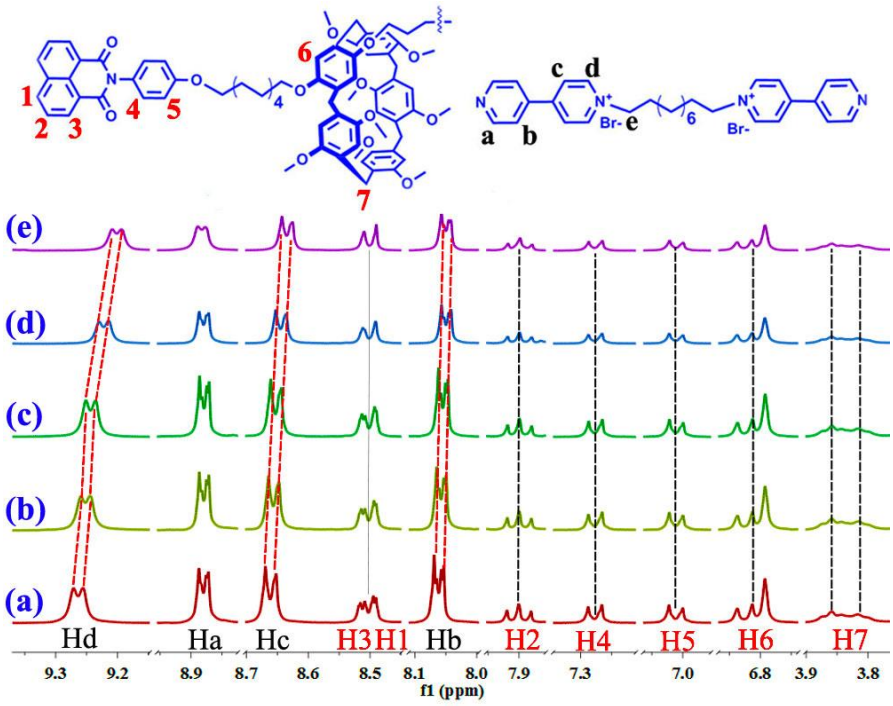

Figure S31. Partial ^{1}H NMR spectra of **SPN-TDPG** in DMSO-d_6 with different equivalent Hg^{2+} (a) 0 equiv.; (b) 0.2 equiv.; (c) 0.5 equiv.; (d) 1.0 equiv.; (e) 1.5 equiv.

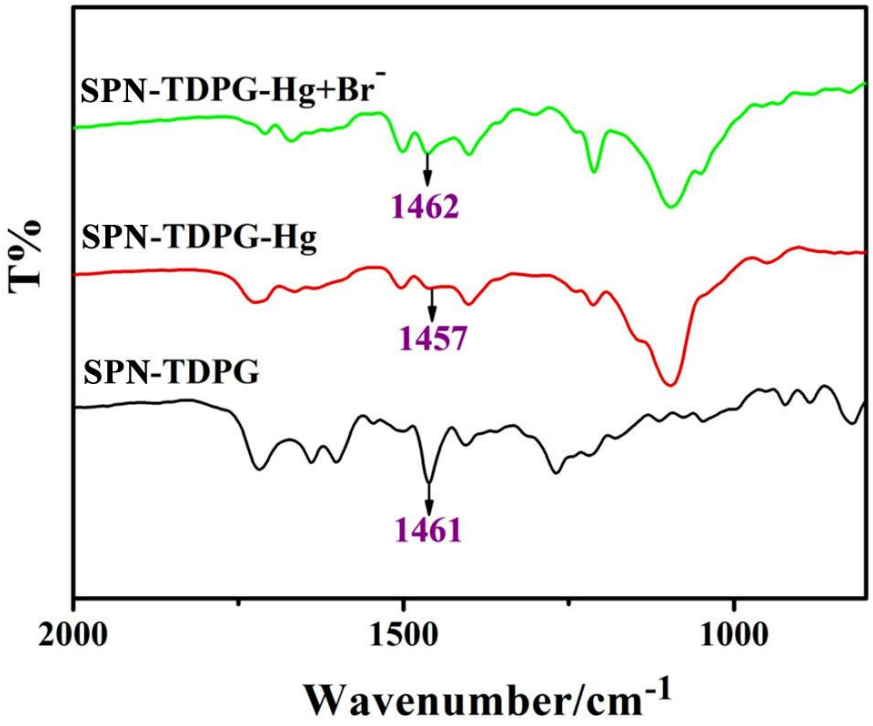

Figure S32. FT-IR spectra of xerogel of **SPN-TDPG**, **SPN-TDPG-Hg** and **SPN-TDPG-Hg** + Br^-.

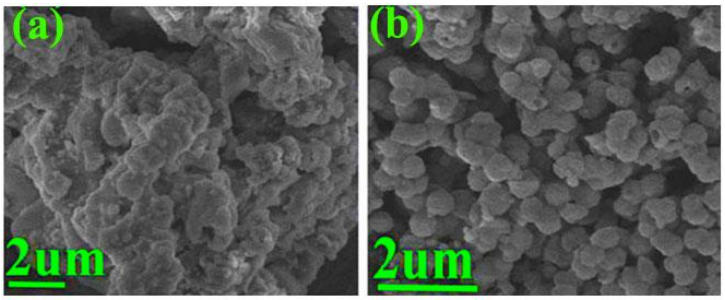

Figure S33. SEM images showing the morphology of (a) **SPN-TDPG-Hg**; (b) **SPN-TDPG-Hg**+Br^-.

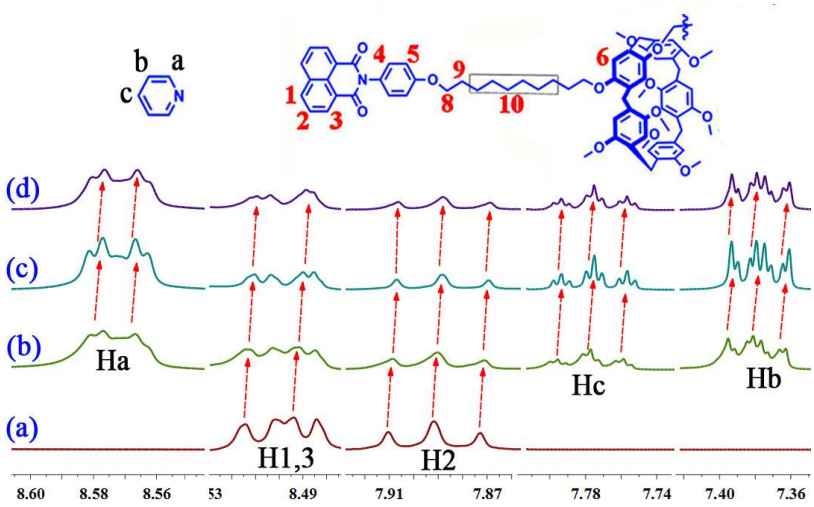

Figure S34. Partial ^{1}H NMR spectra of **SPN-TDPG** in DMSO-d_6 with different equivalent pyridine (a) 0 equiv.; (b) 0.2 equiv.; (c) 0.5 equiv.; (d) 1.0 equiv.

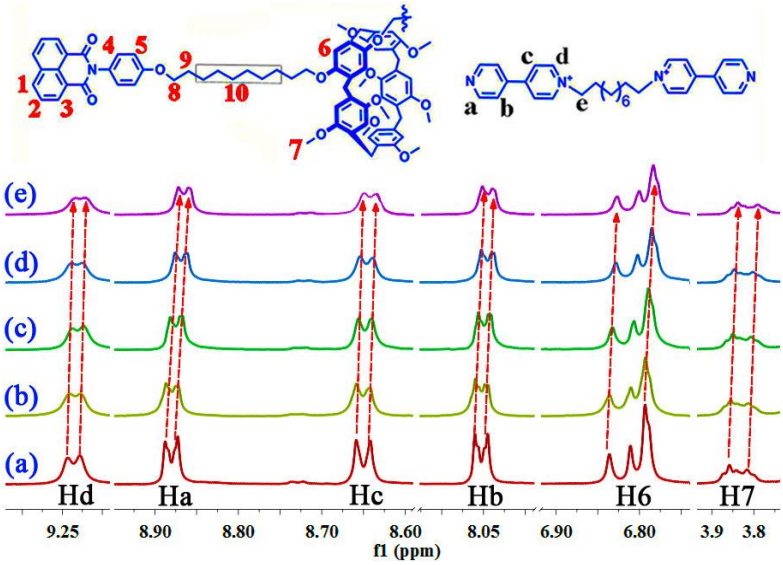

Figure S35. Partial ^{1}H NMR spectra of **SPN-TDPG** in DMSO-d_6 with different equivalent $K_2Cr_2O_7$ (a) 0 equiv.; (b) 0.2 equiv.; (c) 0.5 equiv.; (d) 1.0 equiv.; (e) 1.5 equiv.

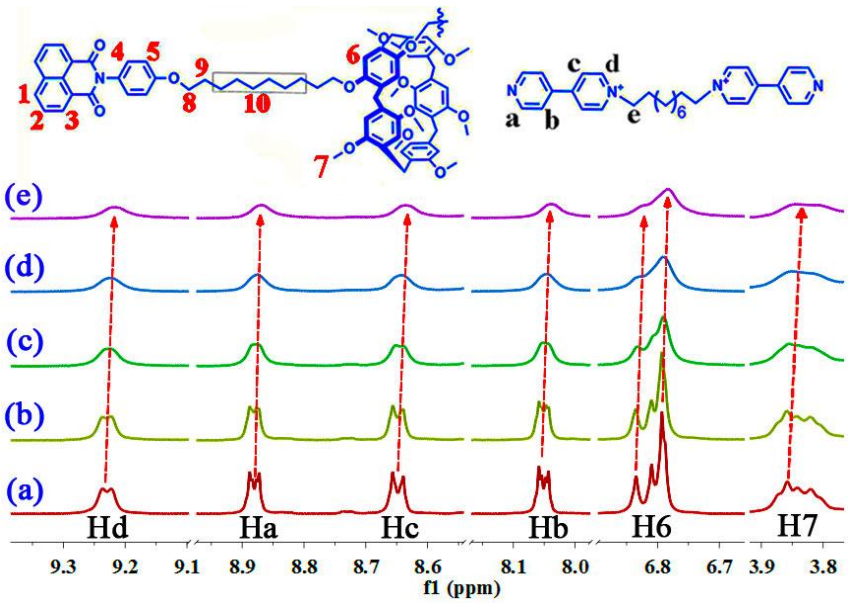

Figure S36. Partial ^{1}H NMR spectra of **SPN-TDPG** in DMSO-d_6 with different equivalent $KMnO_4$ (a) 0 equiv.; (b) 0.2 equiv.; (c) 0.5 equiv.; (d) 1.0 equiv.; (e) 1.5 equiv.

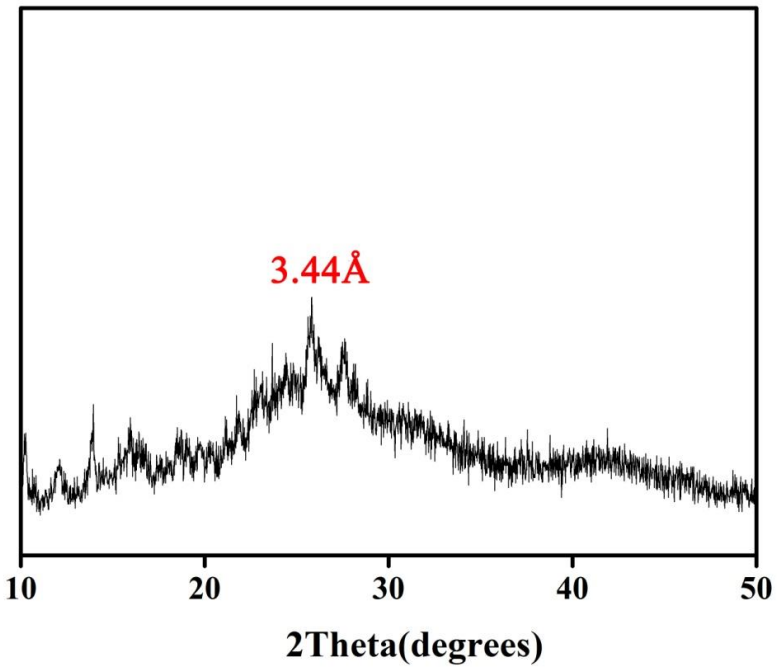

Figure S37. PXRD diagrams of **SPN-TDPG** adsorb rhodamine B.

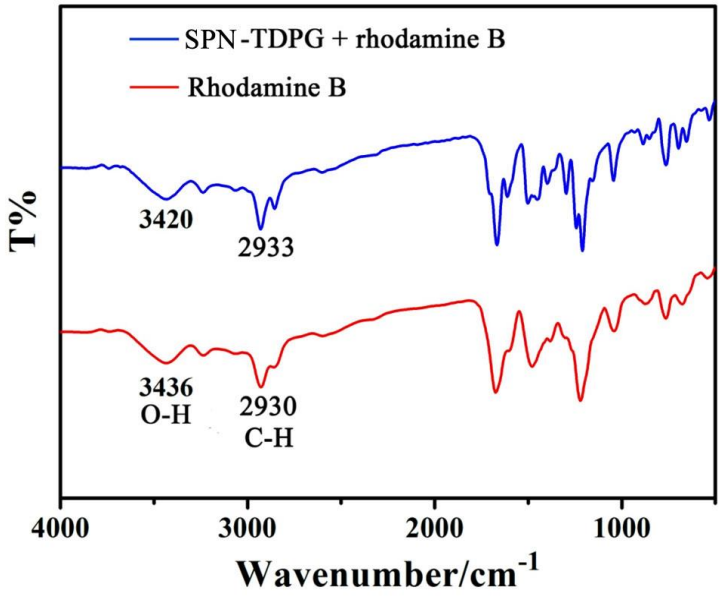

Figure S38. FT-IR spectra of **SPN-TDPG** adsorb rhodamine B.

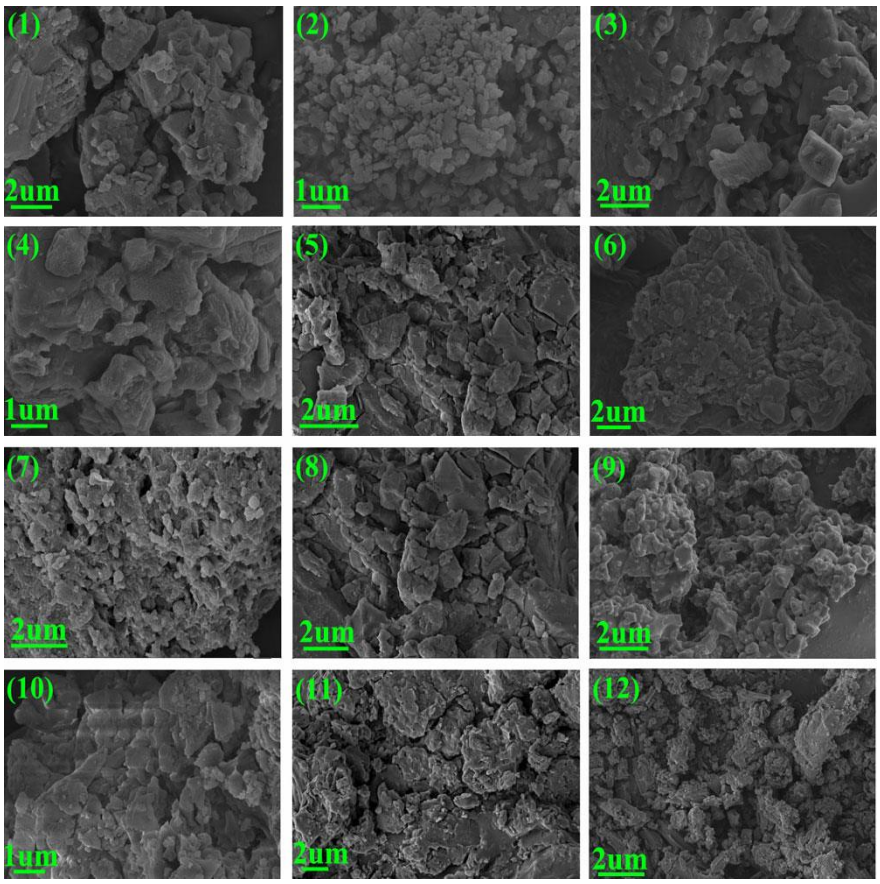

Figure S39. Representative SEM images showing the morphology of **SPN-TDPG** adsorbed (1) methylene blue; (2) bismarck brown Y; (3) giemsa's stain; (4) orangel I; (5) methyl orangel; (6)rhodamine B; (7) sudan I; (8) sudan II; (9) picric acid; (10) 1-naphthol; (11) $KMnO_4$; (12) $K_2Cr_2O_7$.

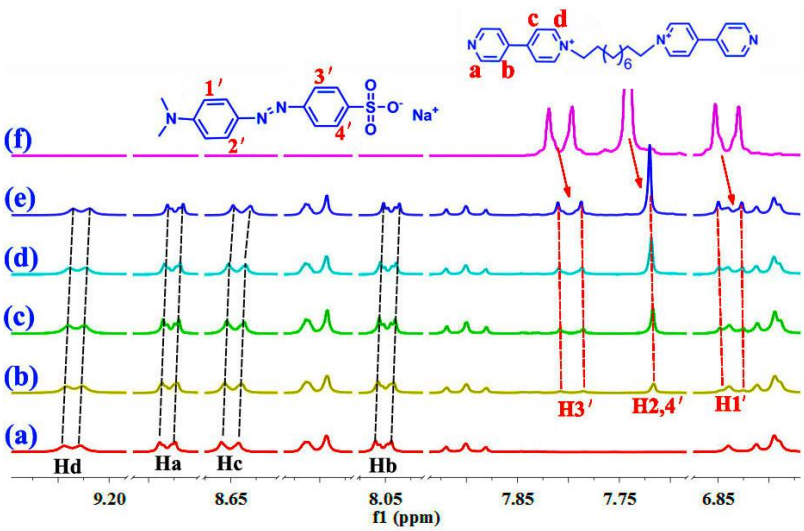

Figure S40. Partial ^{1}H NMR titration spectra (600 MHz, 298K) of 3.0 mM **SPN-TDPG** with various equivalents of methyl orangel in DMSO-d_6 solution. (a) **SPN-TDPG**; (b) 0.5 equiv.; (c) 1.0 equiv.; (d) 2.0 equiv.; (e) 3.0 equiv.; (f) methyl orangel.

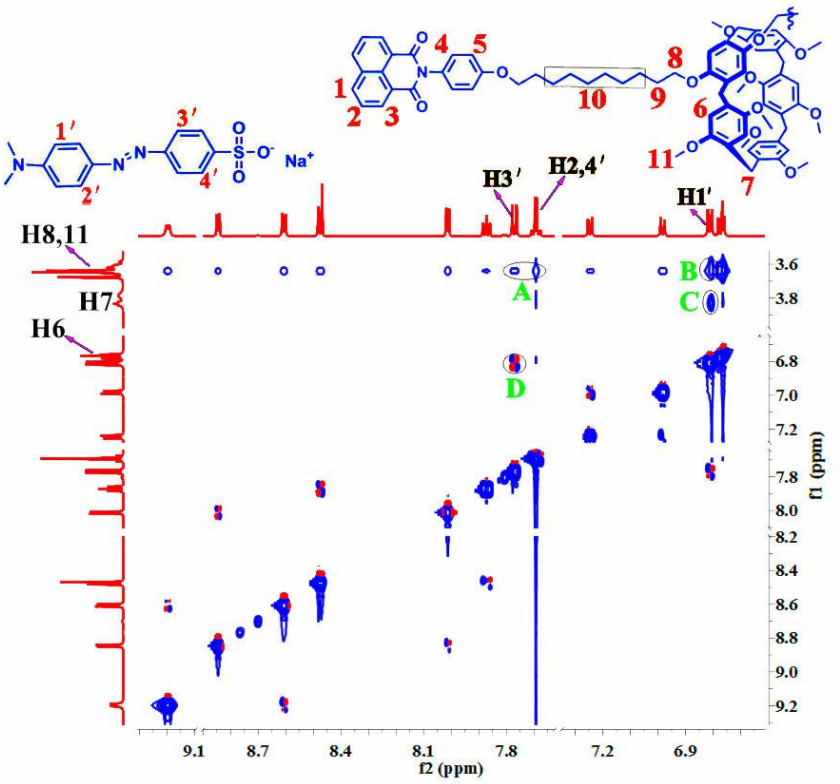

Figure S41. Partial 2D NOESY NMR spectrum of 3.0 mM **SPN-TDPG** and methyl orangel in DMSO-d_6 solution (600 MHz, 298 K).

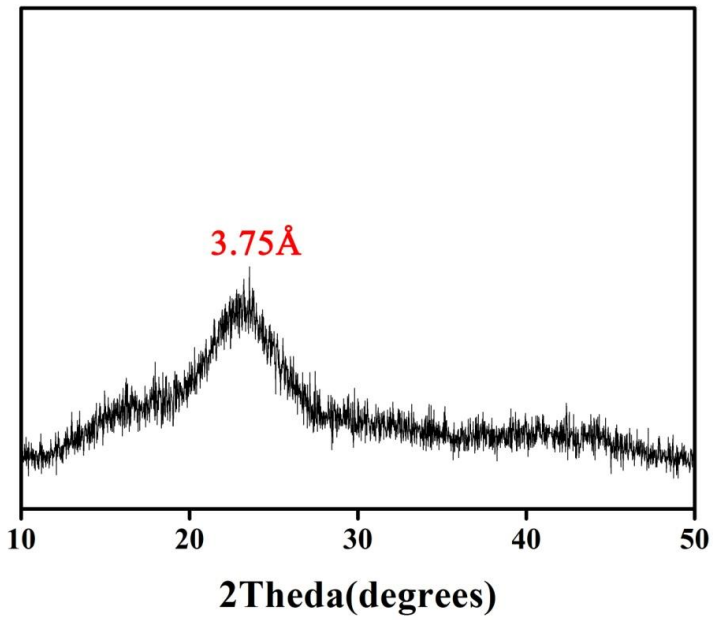

Figure S42. PXRD diagrams of **SPN-TDPG** adsorb methyl orange.

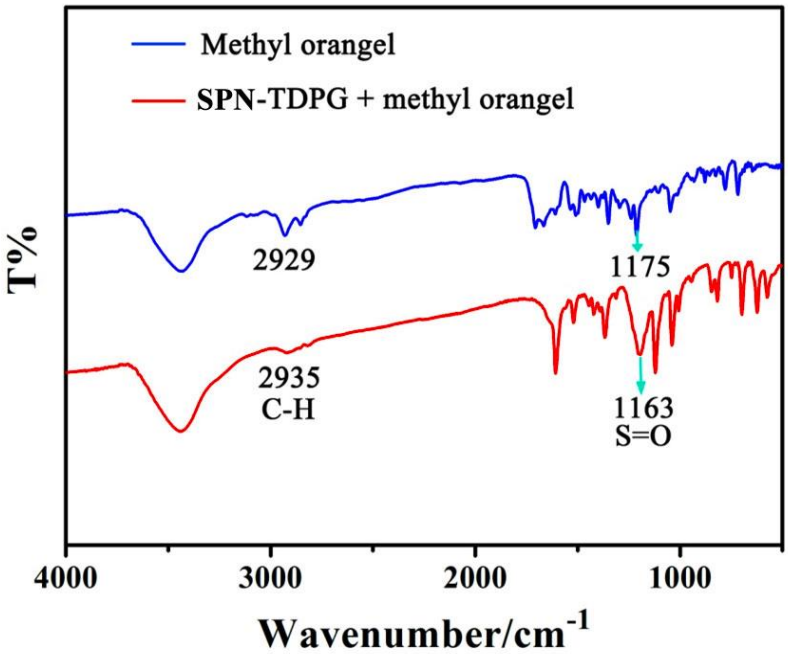

Figure S43. FT-IR spectra of **SPN-TDPG** adsorb methyl orange.

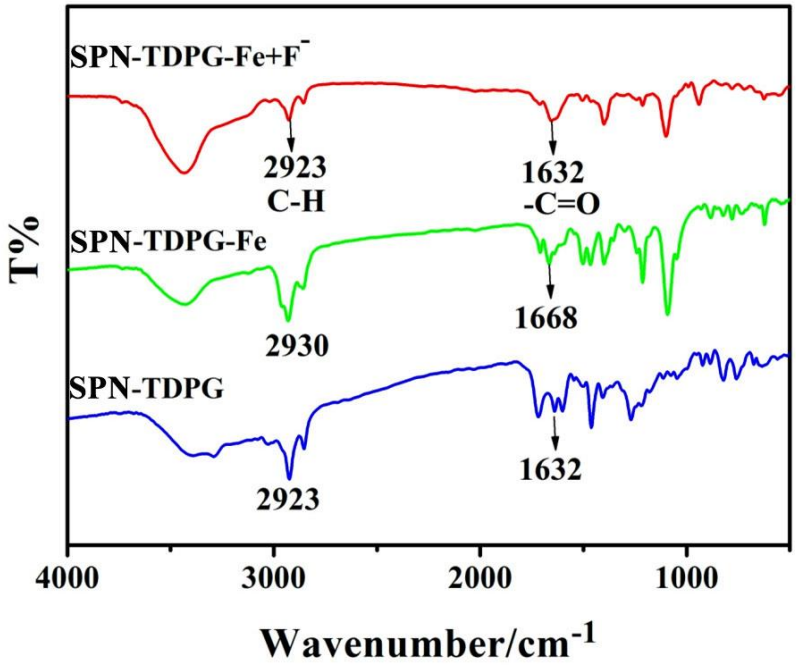

Figure S44. FT-IR spectra of xerogel **SPN-TDPG**, **SPN-TDPG-Fe** and **SPN-TDPG-Fe** + F^-.

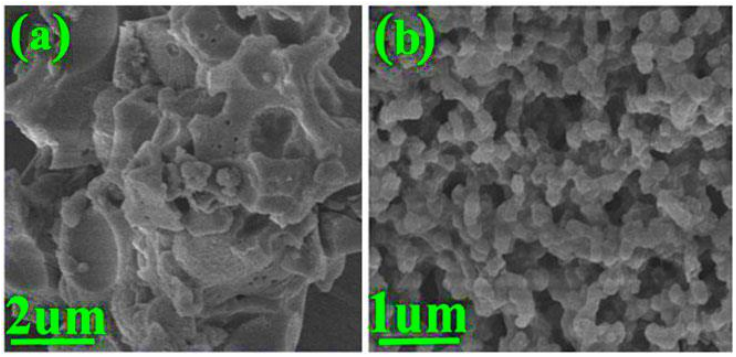

Figure S45. Representative SEM images showing the morphology of (a) **SPN-TDPG-Fe**; (b) **SPN-TDPG-Hg**; (c) **SPN-TDPG-Fe**+F^-; (d) **SPN-TDPG-Hg**+Br^-.